CLAY MINERALOGY AND ITS EFFECT ON PHYSICAL PROPERTIES IN THE GULF OF MEXICO NORTHWESTERN CONTINENTAL SLOPE

A Thesis

by

DEBORA BERTI

Submitted to the Office of Graduate Studies of
Texas A&M University
in partial fulfillment of the requirements for the degree of

MASTER OF SCIENCE

December 2003

Major Subject: Oceanography

CLAY MINERALOGY AND ITS EFFECT ON PHYSICAL PROPERTIES IN THE GULF OF MEXICO NORTHWESTERN CONTINENTAL SLOPE

A Thesis

by

DEBORA BERTI

Submitted to Texas A&M University
in partial fulfillment of the requirements
for the degree of

MASTER OF SCIENCE

Approved as style and content by:

William R. Bryant (Chair of Committee)	Niall C. Slowey (Member)
Wayne Dunlap (Member)	Wilford Gardner (Head of Department)

December 2003

Major Subject: Oceanography

ABSTRACT

Clay Mineralogy and Its Effect on Physical Properties in the Gulf of Mexico Northwestern Continental Slope. (December 2003)

Debora Berti, B.S., Bologna University

Chair of Advisory Committee: Dr. William R. Bryant

The clay mineral composition of sediments deposited in the last six oxygen isotope stages in the Gulf of Mexico continental slope was characterized. Smectite and illite were found to be the two major clay minerals of the clay fraction while kaolinite, chlorite and quartz were present in the clay fraction but in less proportions. Variations in clay mineral abundances, especially in the relative abundances of smectite and illite, were identified in relation to climate changes. Smectite was the most abundant mineral in sediments of the current (stage 1) and last interglacial maxima (stage 5) while illite dominates the clay mineralogy of sediments from the last glacial maximum (stage 2). Relationships between clay mineralogy and physical properties were investigated as well. Significant positive correlations were found between Atterberg limits with the smectite content of the bulk sediment and with clay content. However, the relationship with smectite yielded a significantly higher correlation coefficient. Smectite and clay content also affect the natural water content of sediments and its changes with depth.

ACKNOWLEDGEMENTS

I would like to express my profound gratitude and appreciation to those people who helped me complete my thesis and achieve my master's degree.

Firstly, I thank my advisor and chair Dr. W. R. Bryant for giving me the opportunity to pursue a master's degree, for his relentless encouragement, guidance and financial support. I thank the other members of my committee, Drs. N. Slowey and W. Dunlap, for offering remarkable advice as well as reviewing and improving this manuscript.

I'm deeply indebted to Dr. J. B. Dixon for offering the use of his laboratory and equipment and for his valuable counsel. I also thank Dr. N. White for assisting me with the clay mineralogy analyses and constructively discussing my results. Determination of CEC and total K was made possible by the kindness of B. Brattin who ran the mass spectrometer. Also, I profoundly appreciated the collaboration with T. Tripsanas during my research, especially his input for the sample selection and his updates on the sedimentology.

I am most sincerely grateful to Dan Bean for his tireless support and for his constructive remarks that considerably improved this manuscript.

Sandy Drews offered valuable assistance to get through the intricate bureaucracy of the university.

I am truly thankful to my parents, my sister and my brother for their enouragment and their financial help.

This project was sponsored by the National Science Foundation, in collaboration with Amoco, Chevron, Mobil, Texaco, Phillips, Marathon, Marsco, Inc., GeoTech, Ltd.

TABLE OF CONTENTS

Page

LIST OF FIGURES

FIGURE Page

LIST OF TABLES

INTRODUCTION

In the Gulf of Mexico (GOM) the fossil fuel exploration trend is moving to deeper water, from the shelf to the continental slope and basin, creating the need for investigations of the constraints and problems relating to deeper environments. A comprehensive understanding of seabed processes and hazards can be best achieved by a multidisciplinary approach that integrates seismic, sedimentological, mineralogical, geochronological and geotechnical investigation. Such an integrated program was started in 1998 by the Department of Oceanography at Texas A&M University (TAMU) and the Geomechanical Laboratory at the University of Rhode Island (URI) for the northwestern Gulf of Mexico continental slope. As study area, a 100 km long transect was chosen across the GOM continental slope (Fig. 1) ranging in water depths from 1000 m to 3000 m. Several intraslope basins and a major canyon (Bryant Canyon) characterize the physiography of the area. Based on the results of a high-resolution seismic survey, sediment cores were collected in the area by jumbo piston coring and gravity coring. Part of the cores were used for a geotechnical investigation program conducted at URI, part for a sedimentological, chronological and mineralogical characterization program conducted at TAMU. As part of the TAMU program, this thesis aims at characterizing the mineralogy and specifically clay mineralogy of the sediments and determining how it relates to physical properties.

This thesis follows the style and format of Marine Geology.

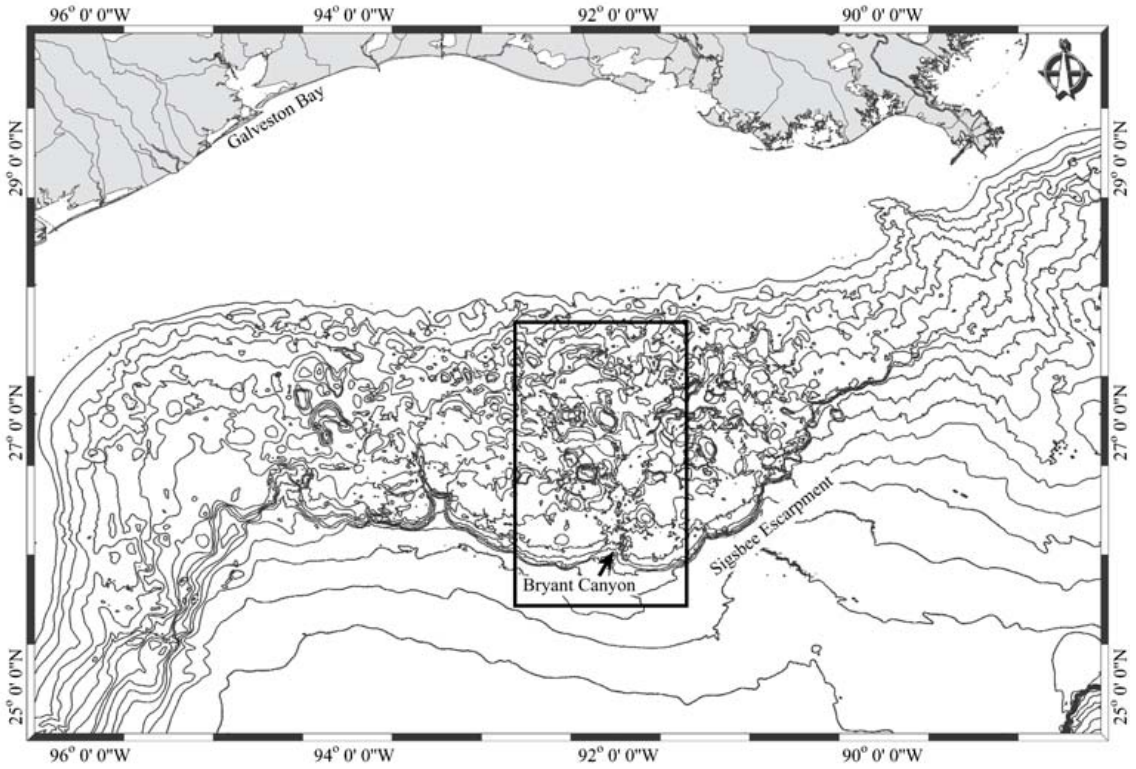

Fig. 1. Location of the Bryant Canyon and study area.

Very few studies have been conducted on the clay mineralogy of sediments of the GOM continental slope and even fewer studies address its variations with depth. As a consequence, there is little understanding of the factors that control such variations, limiting the applicability of the clay mineralogy data available and making their implications uncertain. In this study the clay mineralogy of the Bryant Canyon sediment and its variations with depth and time will be assessed by means of the latest techniques and methods.

Furthermore, knowledge of the clay mineralogy can be of great value for the understanding of soil engineering properties and help explain unusual behavior (Mitchell, 1993). Unfortunately, the extreme complexity of interactions between clay minerals, granular components, organic matter and chemistry of the environment makes the derivation

of universally applicable relationships difficult and uncertain. Correspondingly, attempts to infer clay mineralogy and most of all the presence of minerals problematic for physical properties, based generally applicable relationships often yields deceiving results (Sridharan and Prakash, 1999; Seed et al., 1964; Mitchell, 1993). These uncertainties can however be overcome by establishing less general relationships based on natural samples with well defined applicability and limitations. Accordingly, the effect of clay mineralogy on physical properties in the northwestern GOM continental slope is herein analyzed and, where possible, relations are established. The results and relations will offer a more reliable base to the understanding of physical properties in the GOM continental slope. Most comparisons will be based on Atterberg limits since these limits are widely used for classification purposes, they are relatively independent of depth, and they relate to both composition and other geotechnical properties.

Geological setting

The geology of the northwestern Gulf of Mexico (GOM) continental slope is dominated by the interplay of salt tectonics and sedimentation (Liu and Bryant, 2000; Prather et al., 1998; Bryant et al., 1990). Allochthonous salt massifs, detached from the underlying autochtonous Jurassic salt (Luann Salt), emplaced in the Texas-Louisiana continental slope starting from the Miocene (Prather, 2000; Prather et al., 1998; Diegel et al., 1995). As sediment was transported to the continental slope, salt diapirism lead to the formation of the numerous intra-slope basins and domes. Turbidites and other gravity flows filled the mini-basins during sea level lowstands, while hemipelagic sediments draped the area

during high stands (Bouma, 1983; Lee et al., 1996).

During the Pleistocene, glacial conditions favored an increase in river sediment supply to the continental slope. The large load ultimately led to the eastward migration of the Mississippi River delta that shaped the Bryant Canyon-fan system. The canyon remained active until the end of the penultimate glacial episode (stage 6) when the Mississippi River delta migrating eastward once more (Lee et al., 1996; Tripsanas, 2003; Tripsanas et al., 2000). As the diversion occurred, hemipelagic sedimentation started to dominate the area in concomitance with intense hallokinesis. Salt diapirs formed blockages along the Bryant Canyon creating intra-slope basins and leading to the obliteration of the canyon topography (Lee et al., 1996; Tripsanas et al., 2000; Bouma, 1983). In addition, interdomal intraslope basins formed from coalesced salt diapirs in areas surrounding the canyon (Bouma, 1983).

Bulk density, P-wave velocity and magnetic susceptibility (MS) profiles of the JPC cores collected in the area showed that interbasin depositional environments are continuous across the whole slope (Bryant et al., 2000; Tripsanas et al., 2000). Based on the character of such profiles four units were distinguished in the sediment (Bryant et al., 2000). Successively, more detailed studies added more subdivisions leading to a total of seven units (Fig. 2), relating both to oxygen isotope stages and sedimentary processes (Tripsanas, 2003; Tripsanas et al., 2000).

Specifically, Unit A and E were deposited in the current and last interglacial maxima (stage 1 and 5) and are composed of intensely bioturbated silty clay with abundant forams (Tripsanas, 2003). They are both characterized by extremely low magnetic suscep-

tibility (MS) values (~9 $*10^{-6}$ SI) that reflect a fine grain size and a small fraction of terrigenous sediment. Also sedimentation rates are quite low as well as bulk density magnitude (1.4-1.55 g/cm^3) and depth gradient (Fig. 2). Unit E also includes an ash layer identified as the Y8 ash layer of Kennett and Huddleston (1972) (Elston and Slowey, personal communication).

Unit B and C represent the last glacial episode (stage 5), from its maximum (Unit C) to the deglaciation event (Unit B). An organic matter rich layer marks the end of stage 2, coincident with the Unit A-Unit B boundary. Bulk density linearly rises in this interval from ~1.4 to ~1.7 g/cm^3. Similarly MS increases from ~15 to ~$30*10^{-6}$ SI, indicating a correspondent increase in terrigneous sediment, grain size and decrease in foram content. At the base of Unit C, a drop in bulk density magnitude constitutes one of the most evident stratigraphic marker across the area.

Unit D deposited during stages 3 and 4 which reflect oscillations of smaller magnitude between stage 5 and 2. Foram content and degree of bioturbation are in between respect to those of Unit C and Unit E, although MS is high especially at the top of the unit. High variability in bulk density values conceals its trend with depth.

Finally, Unit F and Unit G deposited when Bryant Canyon was active, during stage 6 (Tripsanas, 2003) and differ from each other for their depositional processes. They consist of turbidity current deposits (Unit F) and laminated silty clay (Unit G). The sedimentological nature of the Bryant Canyon sediments is discussed in great detail by Tripsanas (2003) to whom the reader is referred for further details.

A

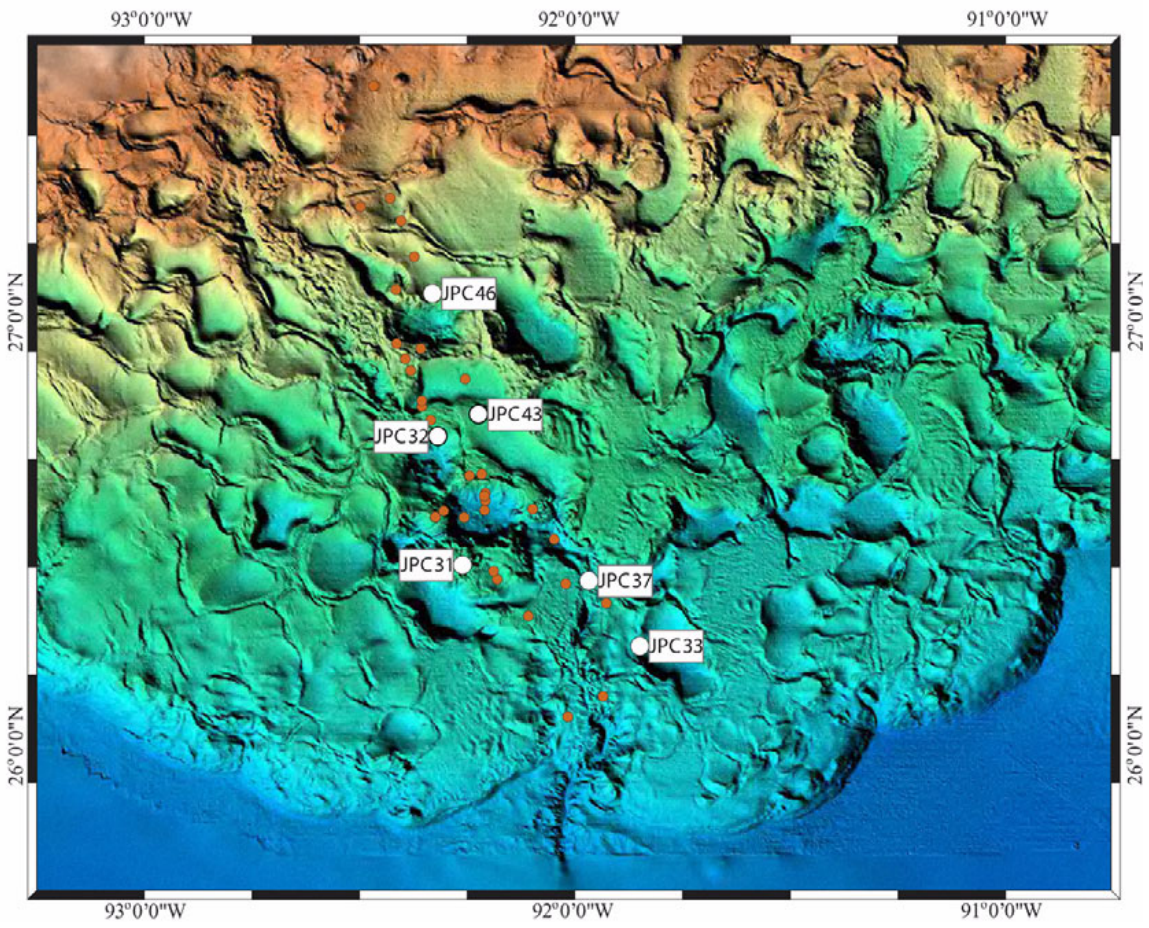

Fig. 2. Continuous character of sedimentation in the Bryant Canyon area. (A) shows the location of the JPC cores collected with red circles whose depth profiles of bulk density and other physical properties show continuity in sedimentation. (B) The bulk density profiles, the sedimentological units and oxygen isotope stages of six cores, whose location is marked by white circles in the map.

B

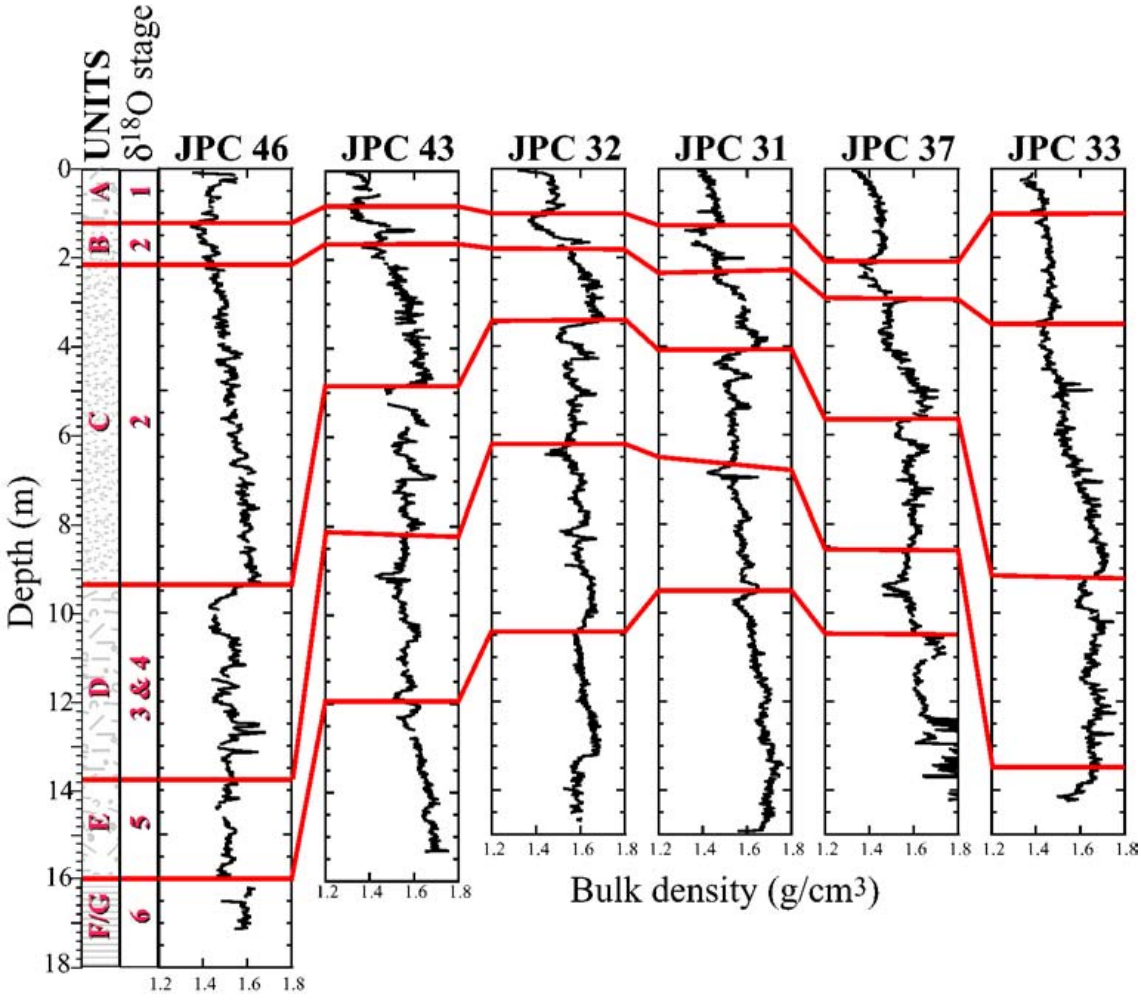

Fig.2 continued

Literature review

Clay minerals in the Gulf of Mexico

Clay mineral studies for the Gulf of Mexico (GOM) mostly focus on shelf sediments and regions close to the major river mouths. Griffin (1962) studied the clay mineralogy of northeastern GOM shelf sediments and related it to their source. He determined that in those areas where the Mississippi River is supplying sediments smectite is the most abundant mineral, followed by illite while kaolinite and chlorite are present in small proportions.

Scafe (1968) and Hottman (1975) studied the clay mineralogy of the northwestern GOM continental slope sediments. They both concluded that smectite is the predominant clay mineral, varying between 60-80%, illite is between 20-30% and kaolinite and chlorite between 10-20% with kaolinite more abundant than chlorite; trace of quartz and feldspars are also present. While the above studies are on surficial sediments, during DSDP Leg 96 the clay mineralogy of an interval of 200 m of sediment from Pigmy Basin was characterized (Ishizuka et al., 1986; Tieh et al., 1986; Stearns, 1985). It is worth noting that the sediment of Pigmy Basin deposited in the same time interval as the sediment from Bryant Canyon used in this study, according to the oxygen isotope stages. While clay mineral abundances obtained by Stearns (1985) and Tieh et al. (1986) differ from those of Ishizuka et al. (1986) their trend with depths agree, as in both cases the smectite to illite ratio decreases below ~50 m but increases once more below ~150 m.

Two different explanations are found in the literature concerning clay mineralogy

variations with depth, relative to intervals of low temperature (<60^{o}C). One addresses chemical-diagenesis driven by the high cation concentration of sea-water (Whitehouse and Jeffrey, 1977; Harder, 1974; Stearns, 1985), the other climate driven changes in rock alteration products hence different composition of river suspended sediment (Weaver, 1977; Brown and Kennett, 1998; Çagatai et al., 2002). Whitehouse and Jeffrey (1977) investigated changes in smectite and other clay minerals when exposed to sea water. They concluded that smectite can transform into illite and chlorite, after fixation of Mg and K in the structure. However, they also predicted that the reaction exhausts fast and may be inhibited by organic matter. Bennett et al. (1999) in a recent study on surficial sediments observed that organic matter is preferentially absorbed by smectite, enhancing the water retention capacity of this mineral. Depth profiles of pore water chemistry, combined with trends of increasing illite to smectite ratio were addressed by authors as evidence of smectite transformation into illite (Stearne, 1985; Tompkins and Shephard, 1979). However the same trends can be explained by changes in sources (Weaver, 1958).

The effect of climate on clay mineral formation is extensively discussed in the literature, due to its implications on atmospheric CO_2 (Kump et al., 2000; Michalopoulus and Aller, 1995). Three main processes related to climate changes directly influence clay mineralogy of sediments: different rates and products of rock weathering, variations in source river drainage basins and distance from the source of terrigenous input. In warm climate chemical weathering is more intense leading to formation of smectite or kaolinite depending on drainage. Oppositely, mechanical weathering prevails in cold climate leading to a clay fraction rich in primary minerals (Dixon and Weed, 1989; Thiry, 1999).

The Mississippi River is the largest supplier of sediment to the GOM northwestern continental slope and to the Bryant Canyon area (Lee, 1996; Prather et al., 1998; Prather et al., 2000). Nonetheless, the extent of the river drainage basin varied in the Quaternary, as a result of capturing of new regions with different geology and climate, and advances and retreats of ice-sheets (Prather, 2000; Brown and Kennett, 1998). A well known instance is the southward extending of the Laurentide ice-sheet during the last glacial episode that covered vast portions of the Missouri and central regions (Prather, 2000; Brown and Kennett, 1998; Prather et al., 1998; Leigh, 1994). Successive melting episodes led to the discharge of large amounts of glacial sediment into the Gulf of Mexico. Oxygen isotope and compositional signals of Plio-Pleistocene meltwater events were recognized in the Gulf of Mexico continental slope sediments by Brown and Kennett (1998).

Lastly, sea-level changes affect the proximity to input sources of terrigenous sediments and the extent of the continental shelves. In the northwestern Gulf of Mexico, during sea-level high stands most of the terrigenous sediment is trapped on the shelf. Sedimentation on the slope is therefore mostly hemipelagic. Conversely, during low-stands rivers drain directly onto the shelf edge and upper slope consequently large amounts of terrigenous sediment reach the continental slope (Liu and Bryant, 2000; Prather et al., 2000; Tripsanas et al., 2000). Correlations between clay mineralogy and oxygen isotope stages have been determined not only for the GOM continental slope (Brown and Kennett, 1998) but also for other regions of the world (e.g. Foucault and Melier, 2000; Jacobs, 1974; Lauer-Laredde et al., 1998; Milne and Earley, 1958; Robert and Kennett, 1994; Robert and Chamley, 1991).

Clay minerals and physical properties

The recognition that clay minerals play a determinant role in the engineering properties of soils and sediments dates back to the early studies of soil mechanics. Buckling of roads, differential settlement of soils under foundations, creep phenomena, excess pore pressure in underwater sediments are examples of problems strictly related to the composition and amount of the clay fraction of the soil.

Clays differ from coarser components of the soil in their characteristic surface electro-chemical properties, arising from their high specific surface area and partially unsatisfied charge (Dixon and Weed, 1989). While coarser minerals possess a definite boundary with the external environment, clays possess an exchange boundary and their behavior is determined by processes acting at the boundary between particle and surrounding environment. A concise review of clay minerals can be found in Appendix A. Clays tend to surround and coat larger particles and if present in sufficient amount they can prevent contact between coarser grains (Mitchell, 1993). Fabric studies on clay-silt mixtures revealed that silt particles float in a clay matrix even for clay contents of 25-30% (Mitchell, 1993; Bennett et al., 1981). Since the behavior of fine grained sediments is mostly determined by the composition of their clay fraction, the understanding of the composition and the properties of such fraction is of key importance.

Numerous studies have been conducted to determine the complex relationships between clay minerals and engineering properties. In general smectitic soils have a higher compressibility, lower permeability, higher shrink swell-potential and lower shear strength than illitic than kaolinitic soils (Mitchell, 1993). Even though the above relation-

ships are valid in general, a wide variation in engineering properties may occur for the same clay mineral, depending on the physico-chemical properties of the pore fluid (Sridharan and Jayadeva, 1982; Abdullah et al., 1999). The effect of pore water chemistry is greater on minerals like smectite that are characterized by uneven charge distribution of the surface, due to imperfections in their structure. A discussion of the effect of pore water chemistry on the physical properties of clay minerals can be found in Mathew and Rao (1997), Sridharan and Jayadeva (1982), Sridharan and Prakash (1999), Sridharan et al. (2002), Mitchell (1993), Bennett et al. (1981).

One way for clays and clay minerals to influence physical properties is by increasing sediment porosity and its capacity to retain water or other fluids. Consequently, the water content of sediments changes as a function of composition even under the same effective stress. The attempt to define water content-behavior relationships led to the definition of the Liquid (W_L) and Plastic (W_P) limits, first introduced by Atterberg and then standardized by Casagrande (Skempton, 1970; Mitchell, 1993). The W_L is defined as the water content at which sediment consistency changes from that of a viscous fluid to plastic, while the W_P is defined as the water content at which sediment consistency changes from plastic to solid. The difference between W_L and W_P is defined as the plasticity index (I_P) (ASTM D4318).

Terzaghi (cited by Mitchell 1993) soon noticed that the results of the Atterberg limits depend on the same factors which determine the strength and the permeability of soils, only in a far more complex manner. Such an observation started a series of studies aimed at identifying the relations between Atterberg limits, compositional factors and

engineering properties of soils. Correlations have been established with swelling and shrinkage properties, compressibility, permeability and shear strength (e.g. Mitchell, 1993; Burland, 1990; Sridharan, 1986; Skempton, 1970). At the same time, studies have been conducted aimed at identifying the mechanisms controlling Atterberg limits, hence physical properties. Clay content has been shown to influence Atterberg limits, and other factors held constant a linear relationship can be established between the two (Seed et al., 1964; Al-Shayea, 2001). Clay mineral type has been shown to be a determinant factor on the liquid limit which increases from kaolinite to illite to smectite (Sridharan, 1986; Lambe, 1960). Nevertheless, complex non-linear interactions between clay minerals and coarse grains, the effect of chemical environment and variability in composition of clay minerals make it extremely difficult to establish relationships of general validity (Mitchell, 1993). For example, studies conducted by Borchardt (1984) showed that the liquid limit of a smectite soil was 97 after treatment with KCl, but just 70 after treatment with AlCl. Abdullah et al. (1999), based on experimental studies, determined that the liquid and plastic limit varies depending on the exchange cation, decreasing from Na to Ca to K.

Clay mineral information is often obtained by means of the Plasticity chart, introduced by Casagrande and currently adopted as classificatory criterion in the Unified Soil Classification System (ASTM D2487-00). In this chart, sediments are classified based on the comparison of their liquid limit (W_L) and plasticity index (I_P). Two lines divide regions in the chart: the A-line ($I_P = 0.73(W_L-20)$) divides silt from clays, while the U-line ($I_P = 0.9(W_L-8)$) marks the upper limit of W_L and I_P (Mitchell, 1993). In addition, the Plasticity chart is divided in regions of different degree of plasticity based on the W_L. However, the

use of this chart is sometimes extended to the identification of main clay minerals. Accordingly, illitic sediments are located just above the A-line, kaolinitic sediments below the A-line and smectitic soils just below the U-line (Holtz and Kovaks, 1981; Colombo and Colleselli, 1996).

Most of the relations described above and found in the literature are based on the use of synthetic, reconstituted soils, due to the necessity to reduce the number of variables involved (Mitchell, 1993). While this approach allows isolation of single or small groups of variables, it disregards indirect and non-linear interactions between them, as well as the environmental influence. However, when these relations are applied to natural sediments they prove incorrect (Sridharan et al., 1988). Natural soils do not simply represent an assemblage of sand, silt and clay, but also a system, the properties of which depend on the composite effects of several interacting and interrelated factors (Sridharan et al., 1988).

METHODS

Core and samples collection

The cores used in this study were collected by jumbo piston coring during a cruise on the R/V Knorr in the GOM continental slope, during 1998. Coring sites were chosen across the continental slope on the basis of high resolution seismic profiles (Fig. 3).

Once equilibrated to room temperature, the cores were logged for gamma-ray attenuation, P-wave velocity and magnetic susceptibility (MS) by a GeoTech Multi-Sensor core logger (MSCL), at 2 cm intervals. Bulk density and derived properties were calculated from the gamma-ray attenuation by assuming a grain density of 2.71 g/cm^3. An extensive discussion of the use of gamma-ray attenuation to determine bulk density (ρ_b), as well as the underlying theory and assumptions can be found in Boyce (1976), Evans (1965), Wetzel et al. (1990) and Bean (2000). The calibration procedure adopted is described by Bean (2000) and LaRosa (2000). Void ratio (e), natural water content (W_C), and porosity (n) were calculated from bulk density (see Appendix C).

Samples for this study were chosen based on the sedimentological units and the characteristics of the physical property profiles. The purpose of this approach was to maximize the potential of obtaining samples representative of all diverse mineralogical-physical property associations in the sediments.

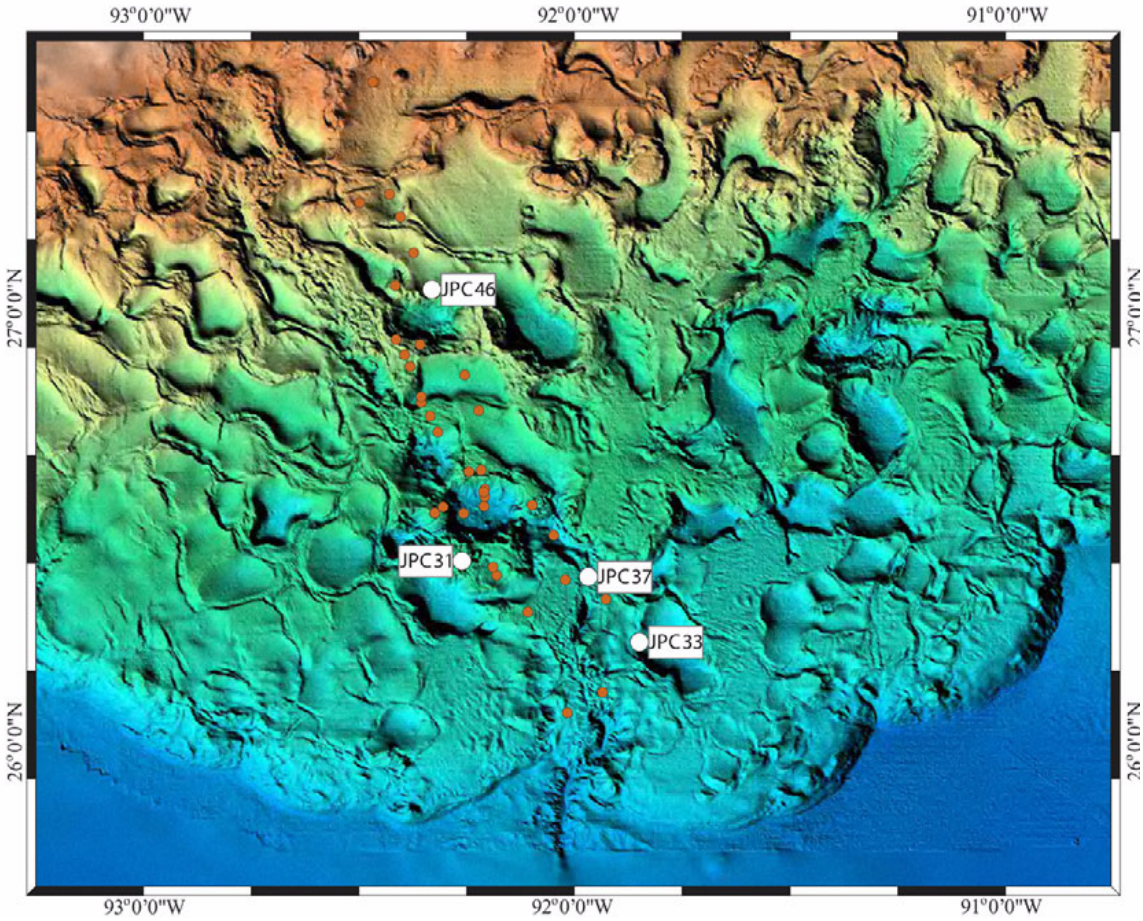

Fig. 3. Location of cores sub-sampled for this study. The dark red circles indicate the location of all the JPC cores collected during the 1998 cruise on the R/V Knorr.

Core JPC 31 (Fig. 3) was chosen for detailed sampling because a comprehensive set of analyses was run on this core that can greatly aid the interpretation of clay mineralogy and physical property results. The analyses include sedimentology as well as oxygen and carbon isotope analyses, additionally a large geotechnical data set was collected at URI in a core close by. Additional samples were collected from cores JPC 46 (upper-slope), JPC 37 (mid-slope) and JPC 33 (lower-slope), in order to investigate spatial as well

as depth variations (Table 1). Units from interglacial maxima (A and E) were only sampled at one location, since transport sorting is more difficult to identify in distal depositional environment.

Table 1

Samples chosen for clay mineralogy-index properties

Sample ID	Core	Depth (m)	Sedimentoligical unit
31-1	JPC 31	0.5	A
31-2	JPC 31	1.8	B
31-3	JPC 31	3.9	C
31-4	JPC 31	5.2	D
31-5	JPC 31	7.6	E
31-5b	JPC 31	9.3	G
31-6	JPC 31	12.8	G
31-7	JPC 31	14.4	G
37-1	JPC 37	13.3	F
33-1	JPC 33	5.0	C
33-2	JPC 33	7.1	C
33-3	JPC 33	12.0	D
46-1	JPC 46	4.8	C
46-2	JPC 46	8.2	C
46-3	JPC 46	12.4	D
46-4	JPC 46	17.1	F

Sampling technique

The purpose of this study is to compare composition to physical and geotechnical properties, it is therefore necessary to obtain geotechnical data and clay mineralogy on the same or comparable samples. While sampling, care was taken not to cross lithologic boundaries

and at the same time, collect a sufficient amount of material to perform both clay mineralogy and physical property tests. Since this study mostly focuses on clay, silt layers/laminas were avoided, except for those that are part of a silty-clay layer (e.g. Unit G). Each sample was divided into three sub-samples, the middle one of which was used for the clay mineralogy, the other two for the Atterberg limits. Pipette analysis to determine grain size, was performed on all three sub-samples. The repeating of grain size and Atterberg limits tests on all sub-samples consented to control the homogeneity of samples as well as the precision of the results.

Mineralogy

A quantitative determination of the clay fraction mineralogy was achieved by a combination of X-ray diffraction (XRD) and analytical methods. The mineral composition of the coarser fraction was qualitatively investigated by XRD.

An XRD survey was performed on randomly oriented powder samples prior to any treatment to identify minerals, like carbonates and sulfates, that will successively be dissolved. A powder was prepared by grinding small amounts of sediment to a size smaller than 140 mesh. The powder was front loaded in an aluminum mount and X-rayed by Cu Kα radiation between 2 and 65^{o} 2θ, at a scan rate of 5sec/0.05^{o} 2θ.

Pretreatments and fractionation

Carbonates, salts and organic matter were removed to enable clay particle dispersion. To remove carbonate, samples were heated to 90^{o}C in a pH 5 1N NaOAc solution, following

the procedure described by Jackson (1956). This procedure has also the effect of replacing the exchange cations with Na, which further favors clay dispersion.

The organic matter was removed by treating the samples with a 30% Hydrogen Peroxide solution, as described by Jackson (1956). At the end of the H_2O_2 treatment, the residues were washed out with a pH 10 Sodium Carbonate (Na_2CO_3) solution.

The Na-saturated samples were separated into sand (>64 μm), silt (64-2 μm), coarse clay (2-0.2 μm) and fine clay (<0.2 μm). Sand was separated by wet sieving, while silt, coarse clay and fine clay were fractionated by centrifugation as described by Dixon and White (1999). Silt and coarse clay fractions were oven dried at 40^{o}C, while the fine clay fraction was flocculated by Sodium Chloride (NaCl), dialyzed to remove the salt, and freeze dried. A diagram of the pretreatments and fractionation procedure is shown in Fig. 4.

X-ray diffraction and infrared analysis

Clay mineral identification by X-ray diffraction (XRD) is based on the 001 peak position of iso-oriented specimens, at known cation saturation and temperature. Five treatments were performed for each sample: Mg saturation, glycerol solvation of the Mg saturated specimen, K saturation at 25^{o}C, heating to 300^{o}C of K saturated specimen and heating to 550^{o}C of K-saturated sample. Each sample was scanned by Cu-Kα radiation at a scan rate of 3 sec/0.05^{o}2θ. A scan interval between 2 and 32^{o}2θ was used for the Mg-saturation and K-saturation at 25^{o}C treatments, while an interval between 2-17^{o}2θ was chosen for the

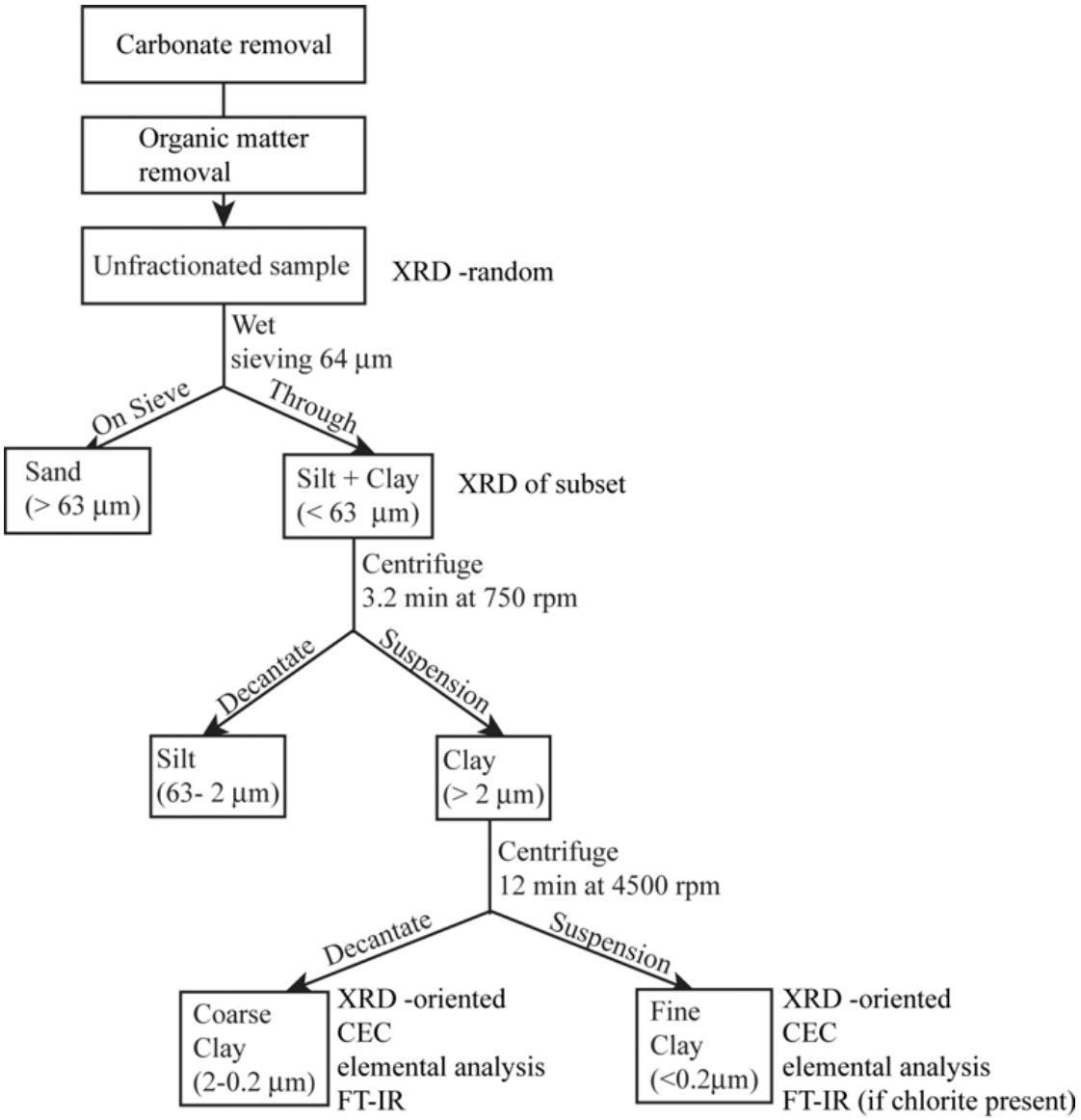

Fig. 4. Pre-treatment and fractionation steps. The tests performed on each fraction are also listed.

other treatments. A correction was applied to compensate the effect of 2θ angle on XRD intensity.

Based on the behavior of the 001 peak after the above treatments clay minerals can be discriminated one from the other. The only exception is discrimination of kaolinite from

chlorite which requires additional testing. The reader is referred to Moore and Reynolds (1989) and Walker (1993) for thorough explanation of clay mineral identification based on their basal peaks (001).

To positively identify kaolinite, a Fourier Transform Infrared Analysis (FT-IR) was performed on chlorite containing samples. In addition, the infrared spectra of clay minerals also carries information about octahedral site occupancies, such as the presence of Fe and/ or Mg and/or Al. A detailed description of FT-IR use in clay mineralogy and molecule studies can be found in Post and Borer (2002) Petit et al. (1998), Acemana et al. (1999). Samples were scanned by diffuse reflectance between 4000 and 400 cm^{-1}, at 0.5 cm^{-1} intervals, against a KBr background. The KBr-sample mixture was prepared by mixing 5 mg of sample to 1 gr of KBr, and kept in a desiccator before testing.

Analytical methods

Cation Exchange Capacity (CEC) and the potassium concentration in the silicates (hereafter referred to as total K) were determined on all coarse and fine clay samples. Replicates of samples and replicates of standard material were tested to ensure the precision and accuracy of results.

The CEC was determined by the Ca-Mg exchange method of Jackson (1956). As standard material a Na-montmorillonite with nominal CEC of 100 cmol/Kg was used. The procedure of Ca saturation and substitution by Mg is described by Jackson (1956). The Ca concentration in the exchange solution is determined by atomic absorbance and converted CEC.

The total K was obtained by means of elemental analysis of silicate minerals. The HF dissolution method of Bernas (1968) was used to dissolve silicate minerals. The method of Bernas (1968) was modified in that the reaction was allowed to proceed at room temperature and the element concentration was determined directly from the nalgene bottles by atomic absorbance.

Quantification of clay mineralogy

In order to minimize the uncertainty of clay mineral quantification, XRD patterns and analytical methods are combined with the aid of the software NEWMOD© (Reynolds, 1985). NEWMOD© is on a one-dimensional diffraction algorithm that simulates intensity and broadness of mineral basal peaks (Walker, 1993). The major innovation that the NEWMOD© software brought relates to the capability to simulate diffracting peak shape and broadening effects due both to instrumental and compositional parameters (Walker, 1993). Particularly, peak broadening caused by characteristic features of clay minerals, like short diffracting domains, mixed layering and thin crystallite can be accounted for (Reynolds, 1989). These parameters exercise a great influence on the shape and intensity of clay mineral peaks consequently yielding large errors in mineral quantification (Kahle et al., 2002). An example relative to shape and intensity of the smectite 001 peak is illustrated in Fig. 5, while a detailed explanation of the theory behind NEWMOD© is found in Walker (1993).

To determine the weight fraction of the minerals composing a sample by XRD pattern simulation a trial and error procedure is adopted, as suggested by Reynolds (1989). However, because numerous variables affect peak intensity, the simulation of a XRD pat-

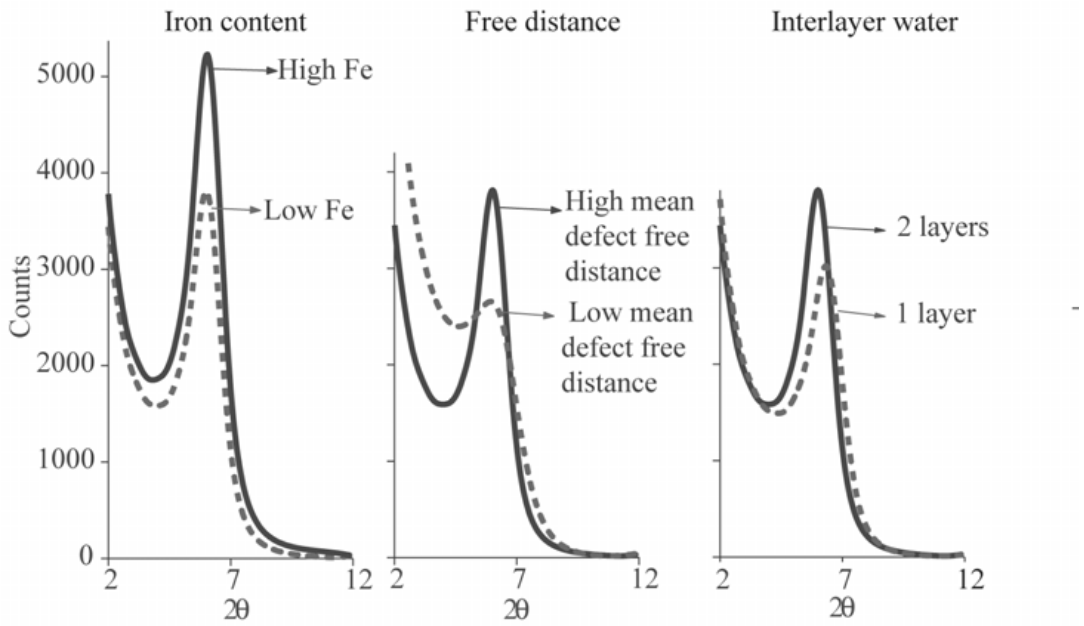

Fig. 5. NEWMOD© models of dioctahedral smectite. Only the 001 peak is shown to illustrate the effect of iron content, free distance between domains and interlayer water. Note the large change in shape and intensity.

tern derived from mineral mixtures has more than one solution (Walker, 1993). To increase the accuracy of the determination, cation exchange capacity (CEC) and clay potassium concentration (total K) were employed.

The determination of CEC allows to pose limits on the fraction of expandable minerals, by far the largest contributors to a sample CEC. Experimental studies determined that smectite has a CEC of 100-110 cmol/Kg (Alexiades and Jackson, 1966); illite of 15 cmol/Kg and kaolinite and chlorite of 3-5 cmol/Kg (Ma and Eggleton, 1999). Smectite contribution to a sample CEC is therefore an order of magnitude higher than that of illite, kaolinite and chlorite. If, for instance a sample has a CEC of 60 cmol/Kg it cannot contain more than 60% or less than 50% smectite (assuming smectite CEC = 100 cmol/Kg).

Concentration of K relates to the amount of illite, since this is the most important,

and often only K-bearing mineral of the clay fraction. To calculate the illite content from the total K, assumptions need to be made about the K_2O content of illite and absence of other K-bearing minerals. In reality, small amounts of K-feldspars are often present in coarse clays and smectites can contain some K in their lattice hence leading to overestimating illite. Furthermore, the K_2O content of illite has a range of variation of 20% (Dixon and White, 1999). In spite of the limits just described, the information brought by analytical data extremely improve the accuracy of XRD based clay mineral semi-quantification. A more detailed explanation of the uncertainties associated with procedures for clay mineral quantification can be found in Walker, 1993 and Kahle et al., 2002.

Index properties

Bulk density, P-wave velocity and magnetic susceptibility and derived variables of the samples were obtained from logger data (See "Core and samples collection" on page 15).

Undrained shear strength (S_U) was measured in the horizontal direction on split cores at 5 cm intervals. The test was performed in compliance with ASTM Standards D4648 (ASTM D4648-94), by means of a motorized miniature vane device with a torque spring. Care was taken to perform the test soon after the core was split, before any loss in water content. Nonetheless problems of moisture loss occurred in the bottom 4 m of core JPC 31 and the correspondent data had to be discarded.

The Atterberg liquid (W_L) and plastic (W_P) limits were determined according to the ASTM standards (ASTM 4318-98). Water contents were corrected for a salinity of 35

ppm, that is the same salinity assumed in the natural water content calculation. The limited number of samples imposed by the complexity of the mineral tests performed raised the need to control for the quality and repeatability of the physical property tests and for the actual sample homogeneity. To achieve this, replicate of samples were used both for Atterberg limits and grain size analysis.

Prior to grain size analysis the samples were treated with a 30% hydrogen peroxide solution to remove organic matter and other binding agents (See "Pretreatments and fractionation" on page 18). To further aid dispersion the samples were left overnight in a 0.1 N Sodium Hexametaphosphate solution. Sand fraction was determined by wet sieving through a #200 (64 μm) sieve. The sand collected from the mesh was washed with distilled water and oven dried at 105^{o}C for at least 24 hours. Silt and clay percentages were obtained by pipette analysis, according to Folk (1974).

RESULTS AND DISCUSSION

Profiles of physical properties

The Atterberg limits of the samples and the undrained shear strength (S_U) of the cores are illustrated in Fig. 6, along with the natural water content (W_C) and P-wave velocity profiles determined by the use of the MSCL. Water content was calculated from bulk density, assuming a constant grain density and 100 % saturation (Appendix C). A consequence of this calculation is that the derived water content profile with depth is a mirror image of the bulk density depth profile. Similarly, void ratio and porosity are calculated from the water content based on the same assumptions of constant grain density and saturation thus yielding a profile with depth similar to that of water content.

In Fig. 6 it is possible to compare the natural water content with the Atterberg limits to gain insights about the consistency of the sediment. The very soft nature of the sediment is reflected in the very high water content that is higher or equal to the liquid limit throughout most of the depth interval studied. The shift from a water content higher than liquid limit to a water content equal to the liquid limit seems to correspond with the base of Unit C. Water contents lower than liquid limit, though higher than plastic limit, only occur below 10-15 m of sediments. Another observation that emerges from the plots of fig. 6 is that Atterberg limits and liquid limit in particular, change considerably between sediments of different units. For instance, Unit C is characterized by the lowest liquid limit in all cores whereas Unit A is characterized by the highest liquid limit.

The high water content and softness of the sediment are also reflected in the P-

wave velocity that reaches values even lower than that of water in the top meters. With increasing depth and decreasing water content, P-wave velocity increases approximately linearly from values of ~ 1470 m/s to ~ 1550 m/s. Similarly, undrained shear strength (S_U) increases approximately linearly with depth from values of ~ 2-3 kPa to ~ 25-30 kPa. Throughout units A, B and C, S_U values are extremely low and increase with depth at a rate as low as 0.4 kPa/m. This trend abruptly changes at the boundary between Unit C and Unit D, coincident with an abrupt shift to greater S_U magnitude. The offset ranges between 5 to 10 kPa, being higher in cores where Unit C is thicker. Throughout the units below, S_U values increase at a faster rate with depth, ranging between 1.6 and 2.4 kPa/m, and are characterized by higher variability. Undrained shear strength, P-wave velocity show similar relations with depth as they are similarly affected by consolidation, stress history and composition of the sediment.

Skempton (1970) determined that the ratio between S_U and effective vertical stress (P_0) is a function degree of consolidation and composition of sediment, the latter expressed by the plasticity index (Ip). For normally consolidated (NC) sediments the following relation is valid:

$$\frac{S_u}{P_0} = 0.0037 \cdot I_p + 0.11 \qquad 1)$$

Based on the range of I_P values obtained, the S_U/P_0 ratio corresponding to the NC state in these sediments varies between 0.2 and 0.3, a common range for soft sediment (Burland, 1990; Skempton, 1970). The effective vertical stress can be calculated from the

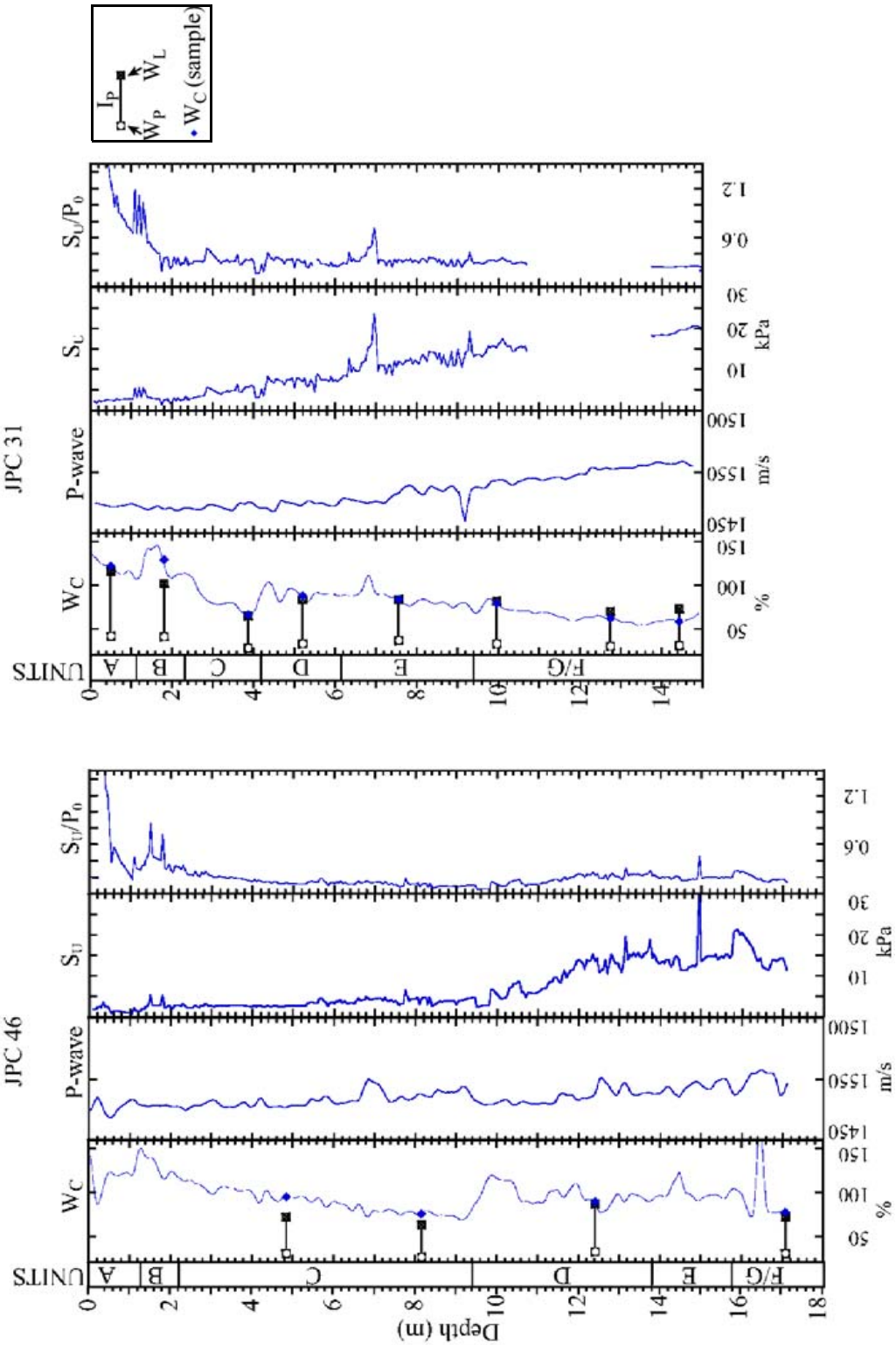

Fig. 6. Physical property profiles of cores. The natural water content depth profile from MSCL measurements (W_C) is compared with liquid limit (W_L), plastic limit (W_P) and plasticity index (I_P). In addition plots of P-wave velocity (P-wave), shear strength (S_U) and shear strength-vertical stress ratio (S_U/Po) with depth are shown.

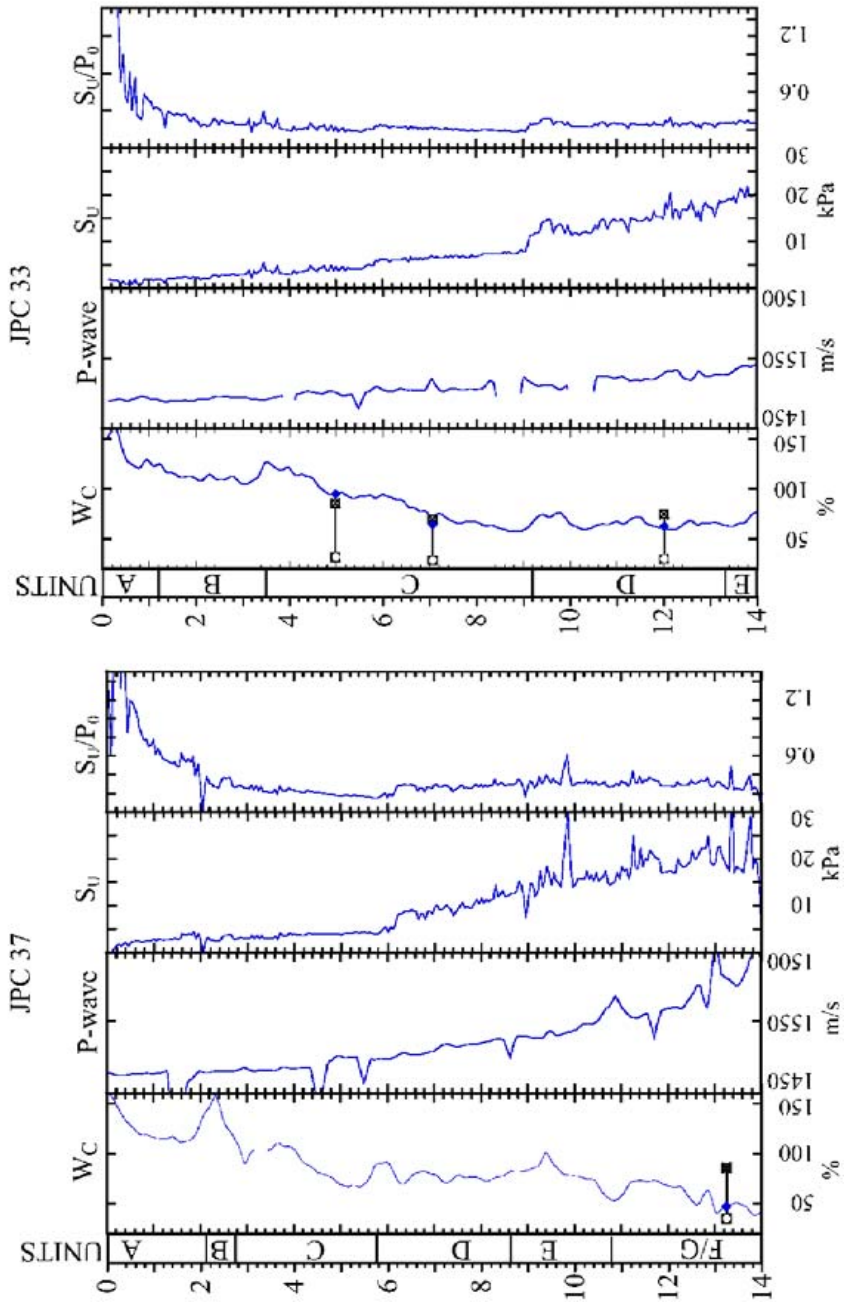

Fig. 6 continued

bulk density data assuming hydrostatic conditions, according to the equation:

$$P_0(h) = \int_h (\rho_b - \rho_w) g \, dh \qquad 2)$$

Where: P_0 = effective vertical stress (kPa); h = depth (m); ρ_b = bulk density from MSCL (kg/m^3); ρ_w = seawater density (1.024 kg/m^3); g = acceleration of gravity (9.81 m/s^2).

Thus the S_U/P_0 ratio can be calculated and used to estimate the degree of consolidation of the sediments. Although this method is less accurate than consolidation tests, it yields to a continuous profile of the consolidation state. The S_U/P_0 plots of the cores sampled indicate that the sediment is normally consolidated, except for a ~ 2 m interval at the top that represents the interval of apparent over-consolidation. Apparent over-consolidation refers to the capability of surficial, water rich fine-grained sediments to bear a vertical pressure higher than any experienced (Bennett et al., 1999). This capability arises from the cohesive properties of fine grained sediments where electro-static bonds form between mineral surfaces and between mineral surfaces with water. Surface electro-chemical properties of clay minerals, at the origin of cohesion are concisely explained in Appendix A. Alternatively, an exhaustive discussion of the mechanisms responsible for the development of apparent consolidation is found in Bennett et al. (1999).

Representativeness of samples

In the choice of samples for clay mineralogy, the sedimentological interpretation was adopted as main criterion for collecting samples representative of the various mineral associations. It is assumed that the largest clay mineralogy variations occur between units, rather than within. One way to check the validity of this procedure as well as how well the variability of the sediment is represented, takes advantage of the high resolution data sets obtained by the MSCL of bulk density (ρ_b), P-wave velocity (PW) and magnetic susceptibility (MS), as well as the high resolution vane shear (S_U) measurements. All these variables are related to each other to some extent but are also affected by different factors. Thus, the data distribution in cross plots bares the effect of both interrelations and external variables, overall illustrating the range of variability in properties and composition of the sediment to a greater extent than any single variable depth profile could do. In Fig. 7, cross plots of PW-ρ_b, MS and S_U with ρ_b describe the range of variations in the sediment of the cores sub-sampled for clay mineralogy. The distribution of the sub-samples (large black circles in Fig. 7) appears to well represent that of the data sets hence confirming the validity of using sedimentological units as selection criterion.

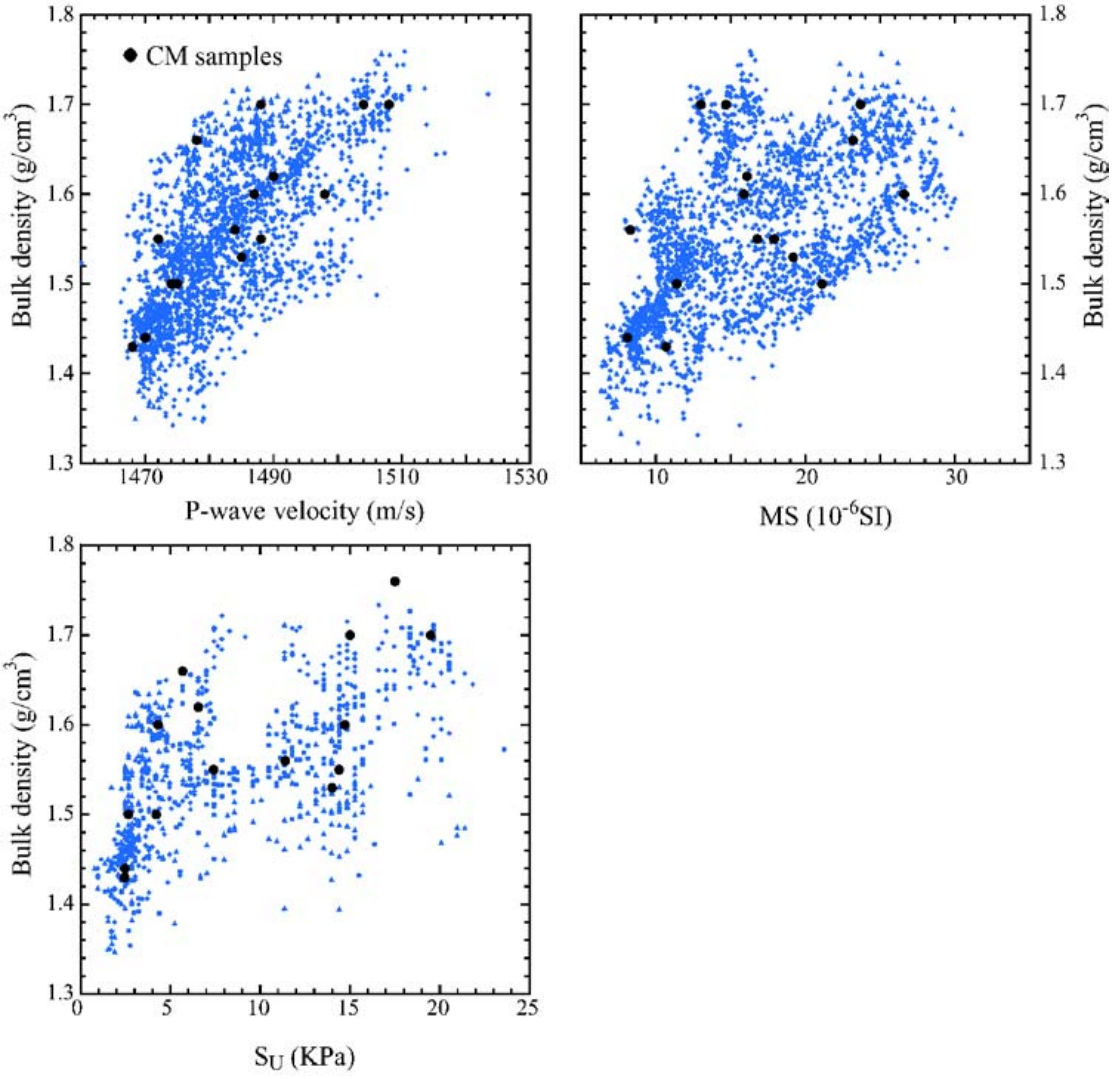

Fig. 7. Cross plots. Plots of bulk density with P-wave velocity, magnetic susceptibility (MS), and undrained shear strength (S_U) of cores JPC 31, JPC 33 and JPC 46 are shown. Data from samples used for clay mineralogy and additional physical property characterizations are marked by large black dots (CM samples).

Mineralogy

Bulk samples and silt fraction

The sediment is mostly composed of silicic-clastic minerals with lesser amounts of carbonates. Among the silicic clastic group, quartz, feldspars, and clay minerals have been identified in all samples, whereas the carbonate group is represented by calcite and dolomite. Quartz and carbonate minerals are those that can be better observed in bulk sample XRD patterns, due to their high degree of crystallinity and consequently intense diffraction peaks (Fig. 8). In most samples, the quartz peak is by far the most intense followed by calcite and dolomite in equal proportions. However, a few samples yield a calcite peak more intense than that of quartz, and a weaker dolomite peak as well. In these sediments, calcite derives from foraminifera shells therefore a more intense XRD peak not only corresponds to a larger calcite content but also to a larger fraction of forams in the sediment. In contrast, quartz is detrital while dolomite can be either of detrital or authigenic origin in marine sediments (Lumsden, 1988). From the analyses conducted in this study the origin of dolomite cannot be positively ascertained. However, a detrital dolomite seems more likely since this mineral is also found in the suspended sediment of the Mississippi River (Griffin, 1962) which is one of the major sources of sediment in the Gulf of Mexico.

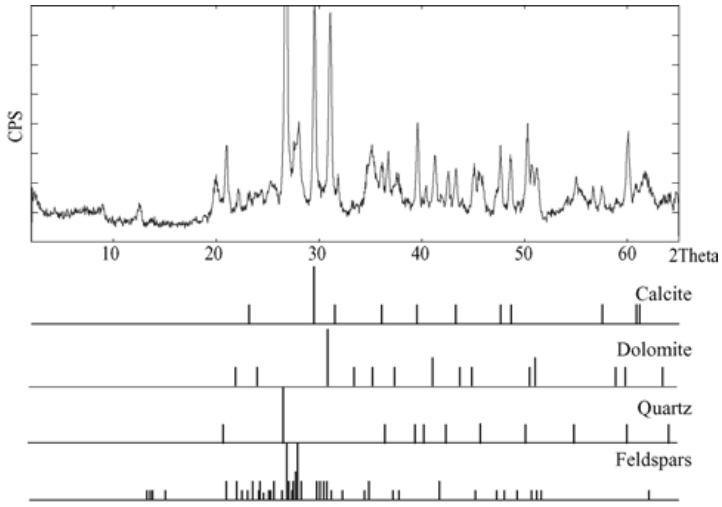

Fig. 8. Example of bulk sample XRD pattern. The pattern is compared to XRD peak positions of composing minerals (JPCDS cards). The quartz main peak has been truncated to better show the pattern of other minerals. Calcite and dolomite determine the two other most intense peaks. Alkali-feldspar, plagioclase halite and clay minerals are the other minerals identified. XRD peak position of reference minerals and interpretation is based on JPCDS reference cards, specifically: quartz from card 5-490; calcite from card 5-586; dolomite from card 11-78; feldspars from card 20-554 (albite) and card 31-996 (ortoclase).

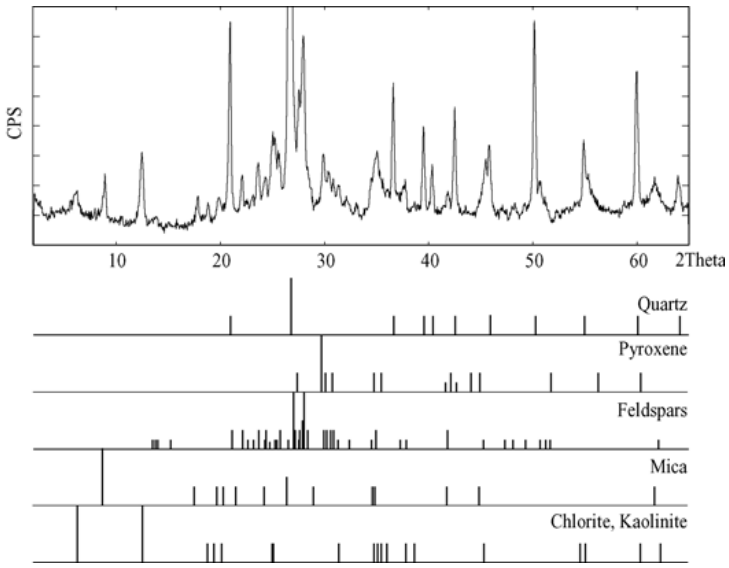

Fig. 9. Example of silt XRD pattern. The pattern is compared to XRD peak position of composing minerals. Quartz, plagioclase, alkali-feldspar, pyroxene (augite), muscovite, chlorite and kaolinite have been identified based on JPCDS cards. The patterns shown in the figure are: quartz from card 5-490; feldspars from card 20-554 (albite) and card 31-996 (ortoclase); mica from card 7-25; chlorite and kaolinite from card 7-78 (clinoclore) and 29-1488 (kaolinite).

To better assess the composition of the coarse silicic-clastic minerals a few silt samples were analyzed by XRD diffraction of random mounts. The analysis was performed on four samples, since differences in the silicate mineralogy of bulk samples appeared small. Such samples were chosen among those with the most diverse bulk mineralogy associations.

Feldspars, pyroxenes, micas, chlorites and kaolinite were identified (Fig. 9). The feldspar group is composed predominantly of albite with a Ca content of about 10% (Smith and Gay, 1958) and orthoclase. Augite (a pyroxene) was identified but the presence of other phases may be masked by the strong overlapping of peaks. Micas are mostly composed of muscovite and illite, with just traces of biotite. Chlorite and kaolinite cause the peaks at 14 Å and 7 Å that were quite intense in some samples. One sample presents an unidentified mineral with main peaks at 2.05 Å, 2.06 Å and 2.49 Å.

Clay minerals

Based on the XRD analysis of oriented clay mounts, smectite and illite are the two most abundant minerals of the clay fraction. Kaolinite, quartz and feldspars were also identified in all samples, whereas chlorite was detected in all samples except for the Holocene one. Since the Holocene is represented by one sample only, it is not certain whether the absence of chlorite is local or widespread.

The presence of kaolinite in samples containing chlorite was verified by infrared spectroscopy. A weak XRD peak at 4.47 Å may be caused by halloysite or chrysotile, the former being an acicular polymorph of kaolinite, the latter of serpentine.

Mixed layer smectite-illite was positively identified in the coarse clay fraction of few samples by the intensification of the 1nm peak after glycerol solvation and the d-space of the first order peak at 19-20 Å. The composition obtained by NEWMOD© simulation, is 70% smectite and 30% illite. Small degree of mixing of illite in smectite and/or of smectite in illite may be present also in other samples, as small degree of interstratification is quite common in soils and sediment but are difficult to recognize by XRD (Weaver, 1977).

As expected, the XRD patterns of the 2-0.2 μm fraction (coarse clay) and of the <0.2 μm one (fine clay) are significantly different (Fig. 10). One of the most apparent differences is the increase in broadness of the fine clay XRD peaks that is caused by smaller size and higher degree of disorder in crystals. Quartz and feldspars cannot be weathered mechanically to the fine clay size due to their hardness whereas chlorite of fine clay size is rare. In contrast, smectite concentrates in the fine clay often constituting the most abundant mineral of this size fraction.

The behavior of the smectite peak after the treatments performed indicates a rather ordered structure. The smectite structure starts collapsing to 10 Å after K saturation even at 25 ^{o}C and, in most cases, completely collapses at 300 ^{o}C, giving rise to a symmetric 10 Å peak (Fig. 10). These characteristics are not commonly seen in soil smectite (e.g. Ohtsubo et al., 2002) which generally undergoes a less complete collapse and yields asymmetric peaks. Most likely this is an effect of the interaction of this mineral with sea-water.

Additional pieces of information about the clay minerals and their characteristics were obtained by fourier transform infrared analysis (FT-IR). As previously mentioned,

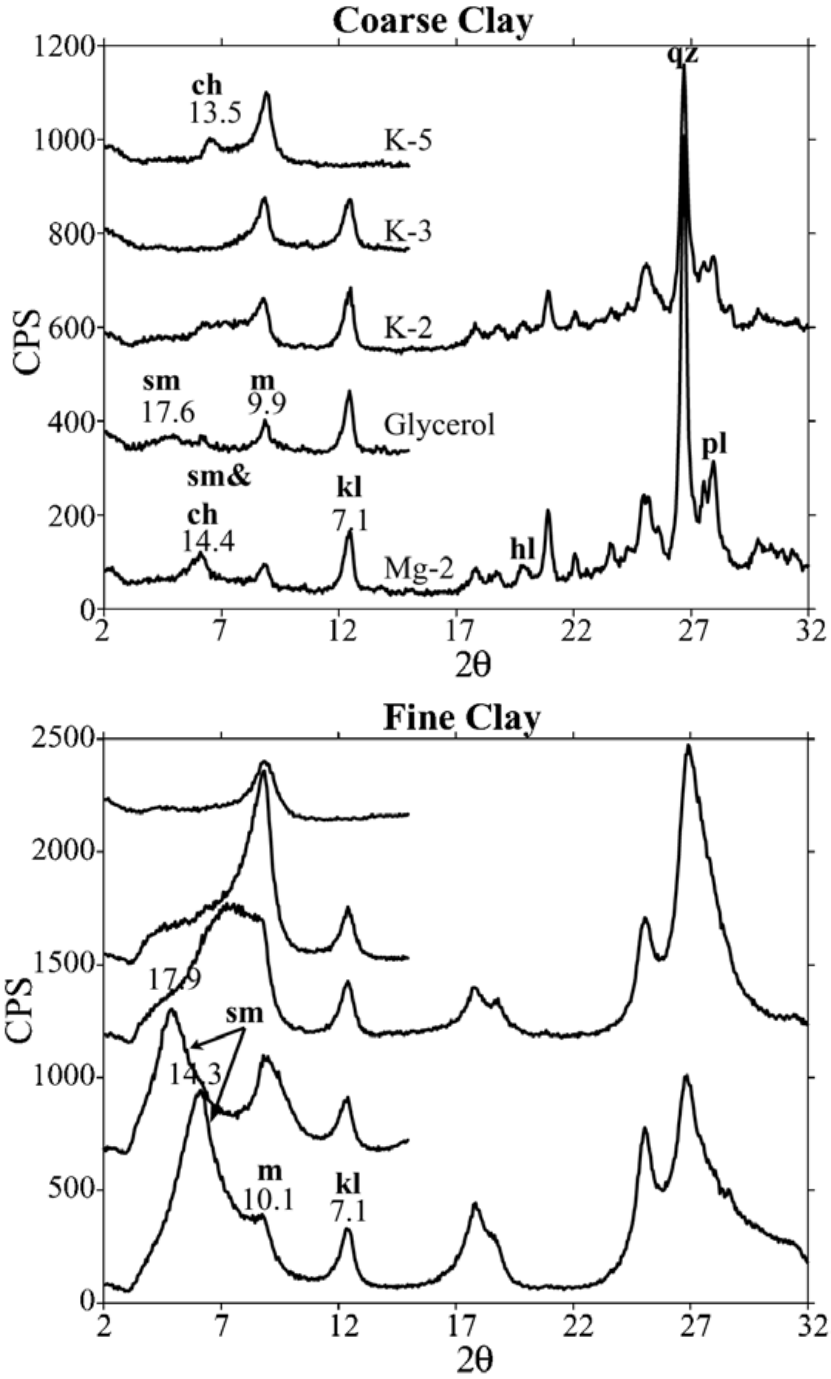

Fig. 10. XRD patterns of coarse and fine clay fractions of a sample. Five treatments were performed, from the bottom: Mg saturation at 25^{o}C, glycerol solvation, potassium saturation at 25^{o}C, potassium saturation at 300^{o}C and potassium saturation at 550^{o}C. **sm**:smectite; **m**: mica (illite); **ch**: chlorite; **kl**: kaolinite; **pl**: plagioclase; **qz**: quartz. Smectite is identified by the peak at 1.4nm in the Mg saturated sample that expands at 1.76 nm after glycerol solvation. Chlorite is identified by the intensification of the 1.4nm peak after heating the K-saturated sample to 550^{o}C.

FT-IR spectra allowed to positively identify kaolinite in samples containing chlorite, by its four characteristic OH stretch bands (Fig. 11). The intense OH-stretch band at 3620 cm^{-1} is due to Al in octahedral sites and indicates that mica and smectite are predominantly dio-ctahedral. Smectites are composed of montmorillonite, the Mg rich phase, but nontronite, the iron rich-phase was also recognized by the absorbance band at 3560 cm^{-1}. Nontronite and iron rich smectite are frequently found in marine sediments and may be of authigenic origin (Cole and Shaw, 1983; Aoki and Kohyama, 1991). As site occupancies are an input parameter in the program NEWMOD, the information from the FT-IR spectra can assist in correctly simulating the XRD peak intensity and shape of clay minerals.

CEC, elemental analysis and quantification of clay minerals

The determination of mineral fractions in the clay is based on CEC, K content obtained by elemental analysis and computer simulation by NEWMOD©.

The CEC and K concentration for the fine and coarse clay fractions as well as their clay average are reported in Table 2. Significantly higher CEC in the fine clay rather than coarse clay fraction is consistent with the XRD results and a consequence of smectite small size. In contrast, K concentration varies more between samples than size fractions. The precision and accuracy were better for the CEC rather than K determination, but very high in both cases.

In order to verify the validity of using CEC data to quantify smectite, this variable was compared to the height of the 18 Å peak of the glycerol solvated XRD patterns and

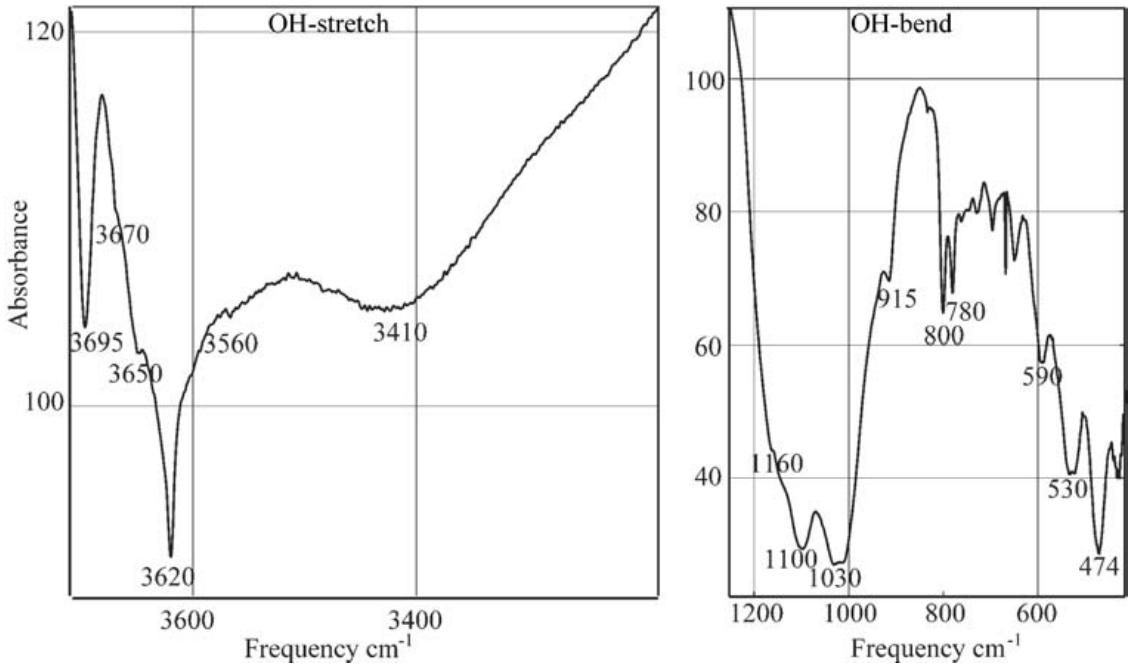

Fig. 11. IR spectra of coarse clay. Only the OH-stretch, and OH bend regions are shown. The rest of the spectra has been omitted because is not diagnostic. In the OH-stretch region (left) absorbance bands at 3695, 3670, 3650 and 3620 cm^{-1} indicate kaolinite. The 3620 cm^{-1} is intensified due to the overlapping of the dioctahedral clays. A band at 3560cm-1 indicates nontronite (iron smectite), while the 3410 cm^{-1} is due to water absorbance by smectite. In the OH-bend region (right) the bands between 1160 and 915 cm^{-1} are due to smectite and illite. Quartz causes the bands at 800 and 780 cm^{-1}, while feldspars produce the bands between 780 and 471 cm^{-1}.

that of the 14 Å peak of the Mg-saturated XRD patterns (Fig. 12). Both plots show a substantial change in slope in correspondence of data from coarse and fine clay fractions. The trend is well represented by an exponential fit that leads to a correlation coefficient (r) of 0.96 and 0.97 for the glycerol solvated and Mg saturated patterns respectively. The best fit equations are not reported because the strong dependence of XRD peak intensity on instrument limits their applicability.

It is important to notice that the correlation was just as good for the glycerol sol-

vated and Mg saturated treatments, despite the overlapping of the chlorite peak in the latter. This is a consequence of the type of chlorite in the samples, characterized by more Mg than Fe in octahedral sites hence a weak first order peak (14 Å) and strong second and third order peaks (7 and 3.5 Å). The relation between CEC and smectite peak height confirms the validity of using this property as smectite indicator and in semi-quantitative analysis.

Table 2

CEC and K

Sample ID	FC CEC	CC CEC	C CEC	FC K	CC K	C K
31-1	67.4	40	56.8	2.77	3.44	3
31-2	61.2	30	46.5	3	4.2	3.7
31-3	49.8	23	37.5	3.9	4.8	4.3
31-4	59.3	30	46.8	2.9	3.8	3.3
31-5	63.6	35.6	52.3	2.7	3.1	2.9
31-5b	56.8	27.6	40.8	1.9	3.4	2.7
31-6	55.8	29	45.7	2.6	3.6	2.9
31-7	55.3	35	45.5	2.6	3.4	3
33-1	64.5	37.9	51.9	2.7	4.2	3.4
33-2	55	35	45	3.1	3.9	3.5
33-3	56	24	42.5	3	3.9	3.4
37-1	57.3	22	39.9	3.2	4.2	3.2
46-1	55	24	40	4.18	4.65	4.4
46-2	49	23	36.9	3.8	4.4	4
46-3	60	27	46.2	2.8	3.9	3.3
46-4	55	31	43.9	2.6	3.3	2.9

CEC and K content of samples and clay average. FC = fine clay; CC = coarse clay; C = clay

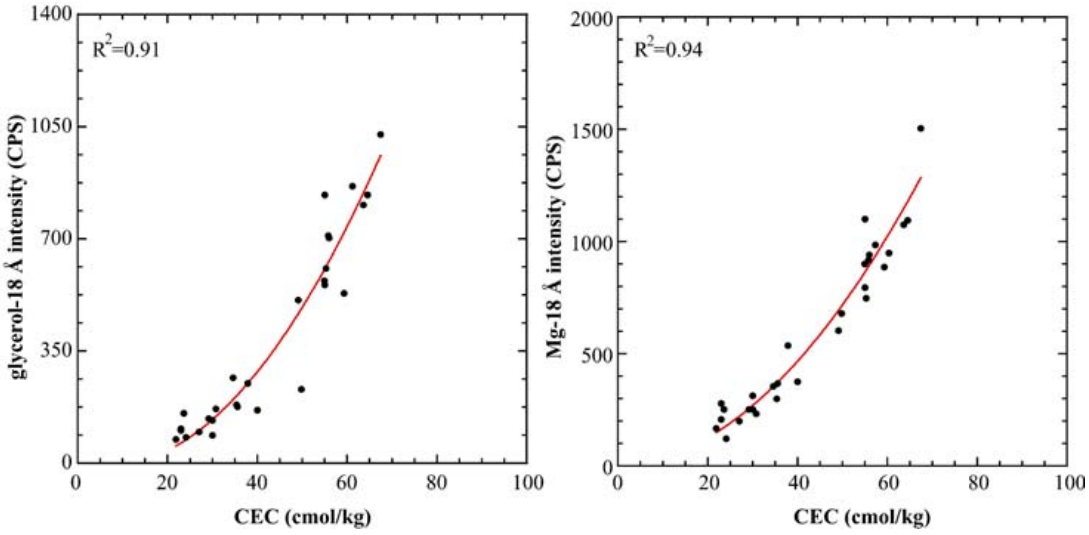

Fig. 12. Correlation between CEC and smectite peak intensity. A good correlation exists between CEC with smectite peak height from the glycerol pattern (left plot) as well as with smectite peak height from the Mg saturated pattern (right plot).

In contrast the correlation between K concentration and peak height yielded a correlation coefficient of 0.7, far less than that found between CEC and smectite peak height. While this may be explained in part by the less precision in the K than the CEC determination, additional and more relevant causes are the variability in illite composition, presence of K-bearing minerals in the coarse clay fraction and the weakness of the illite diffraction peak.

In addition to determining K concentration, a few noteworthy features emerged from the results of the elemental analysis. For instance, iron is more abundant in the fine rather than coarse clay fraction, a consequence of the small size of iron oxides. In contrast, Ca is significantly more concentrated in the coarse clay fraction due to the presence of some plagioclase. Accordingly, samples with more intense plagioclase XRD peaks were

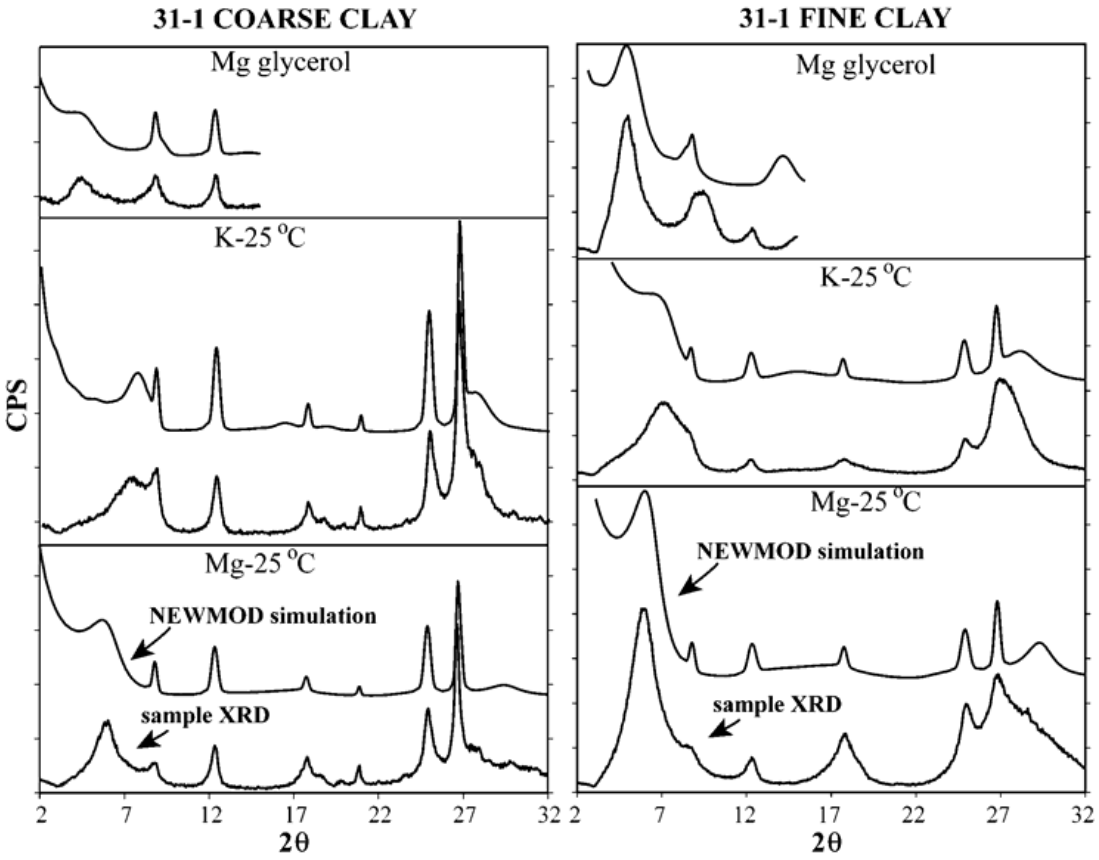

Fig. 13. Comparison between NEWMOD© models and real XRD patterns. The figure shows the coarse clay (left) and fine clay (right) fractions of the same sample. From the bottom of the figure the following treatments are shown: Mg-saturation, K saturation at 25°C and glycerol solvation. The model is always on top of the real pattern.

also richer in Ca. Finally, while the concentration of most elements was relatively similar between standards and samples, Mg was twice as concentrated in the samples, a feature often interpreted as resulting from interactions of minerals with sea-water (Weaver, 1977; Whitehouse and McCarter, 1977).

An example of simulation of XRD patterns by NEWMOD©, compared to the real one is shown in Fig. 13. The XRD patterns obtained after heat treatments of K saturated samples were not simulated since they do not bear quantitative information.

Mineral compositions used for the simulations were consistent both with the information gathered by FT-IR analysis on site occupancies and XRD patterns. In other words, dioctahedral minerals were used, except for chlorite, similarly crystal size and ordering were kept consistent with the shape of XRD peaks. The composition of minerals was held constant between samples of the same size fraction in most cases. Adjustments in crystal size and ordering were instead performed between minerals of the coarse and fine clay patterns

Clay mineral abundances and their variations

The results of the semi-quantitative analysis show considerable variations in mineral abundances between samples. Smectite and illite make up together 75-85% of clay but their proportions vary over a wide range. Likewise, fractions of other minerals vary following the trend of one or the other major mineral. The clay mineral abundances used in this section are referred to the clay fraction, according to Equation 3 and are listed in Table 3:

$$M_C = M_{FC} \bullet (FC/C) + M_{CC} \bullet (CC/C) \quad 3)$$

Where: M = mineral fraction; FC = fine clay; CC = coarse clay; C = clay

One possible cause of variation in clay mineralogy discussed by scientists is early (also called chemical) diagenesis of smectite into illite and chlorite in marine sediments (See “Clay minerals in the Gulf of Mexico” on page 8). Indeed, some analyses indicate structural modifications in smectite and maybe other minerals induced by sea-water. Specific instances are the shape and behavior of the smectite 001 peak after K saturation and

heat treatments, high Mg content revealed by elemental analysis (twice as standard soil) as well as traces of nontronite revealed by FT-IR.

Table 3

Clay mineralogy

Sample ID	smectite	illite	kaolinite	chlorite	quartz and feldspars
31-1	51	32	11	0	5
31-2	40	40	12	3	6
31-3	29	47	10	8	6
31-4	40	37	11	5	7
31-5	47	32	12	2	7
31-5b	34	31	18	5	11
31-6	40	33	16	4	7
31-7	38	34	17	5	6
37-1	33	39	12	5	11
33-1	46	37	11	4	3
33-2	39	38	16	3	5
33-3	35	39	12	5	11
46-1	32	50	9	4	5
46-2	29	46	9	9	6
46-3	39	36	11	5	8
46-4	37	34	19	1	8

Although these are not conclusive evidence of chemical diagensis, they are in agreement with the findings of experimental work by Whitehouse and Jeffrey (1977) on smectite transformation in sea-water.

On the other hand, variations in clay mineral abundances resulted independent of

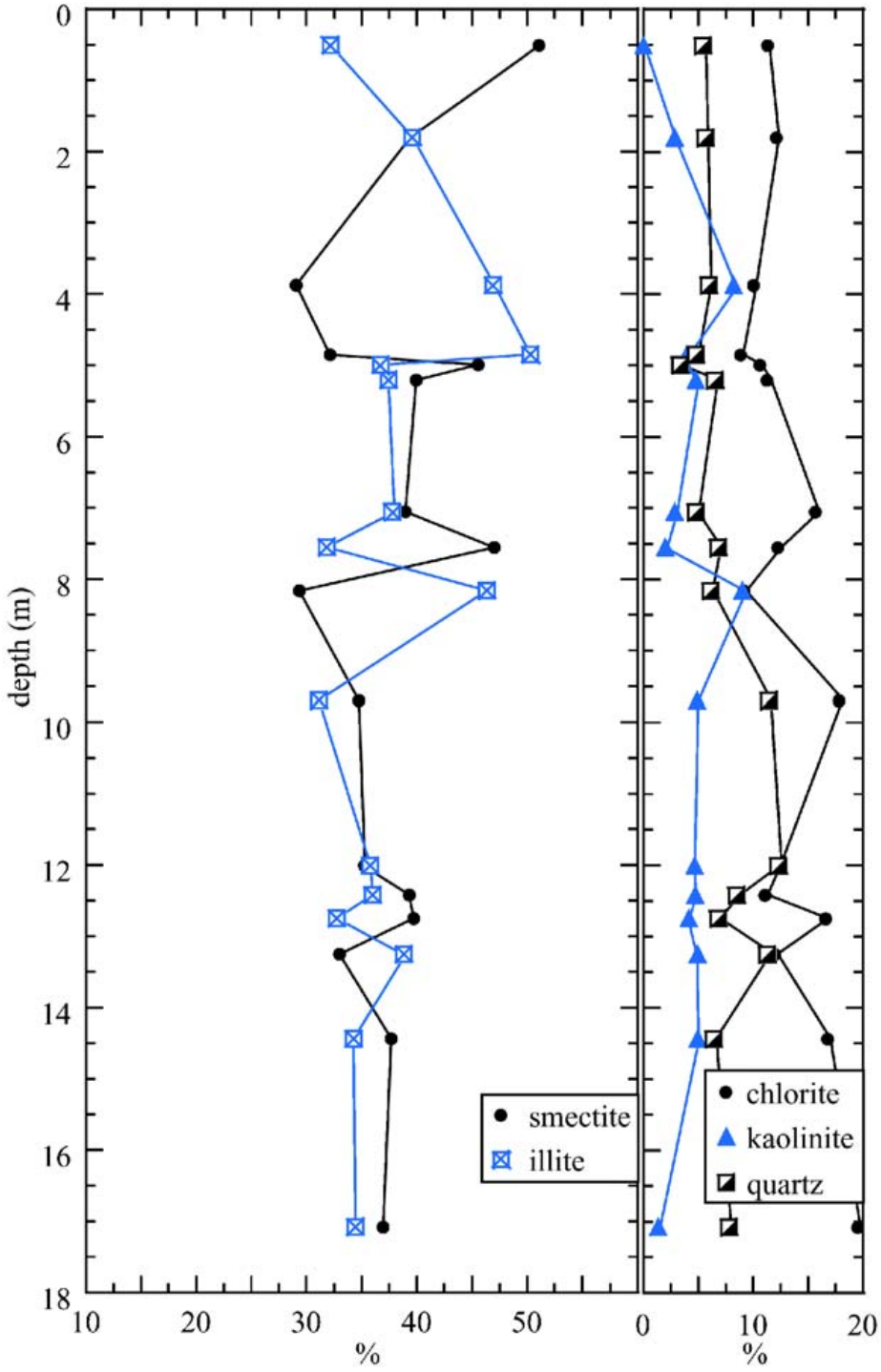

Fig. 14. Clay mineralogy variations with depth. The data refer to mineral abundances in the clay size fraction. Note that variations in mineral abundances do not follow any trend with depth.

depth (Fig. 14) thus disproving formation of significant amounts of illite and chlorite from early diagenesis of a relatively homogeneous precursor clay. Uptake of organic matter by smectite may be inhibiting such transformation (Whitehouse, 1977; Bennett, 1999). Consequently, interaction of sea-water with clay minerals while largely affecting the ordering and structure of crystals does not lead to significant mineral transformations. Nonetheless, the changes in mineral structures observed are likely to leave a mark in the physical properties of the sediment

In Fig. 15 the clay mineralogy profiles of cores JPC 46, JPC 31 and JPC 33 are shown besides lithologic units, water content and clay content. As well illustrated by core JPC 31 where all units were sampled, the clay mineralogy follows a cyclic trend with depth. Such trend is particularly evident for the two major minerals, smectite and illite.

Sediments of Unit A, at the top of the core, are the richest in smectite, and poorer in illite. The smectite fraction rapidly drops to reach its minimum in Unit C whereas the illite fraction reaches its maximum. In Unit D and Unit E smectite content rises once more, reaching another maximum, though not as high as at the top of the core (Fig. 15). Illite decreases correspondingly. Unit F/G is characterized by a quite uniform composition with approximately same proportions of smectite and illite, similarly to Unit B and Unit D. However, at the top of this unit in correspondence of a change in color from greenish-gray to brownish-red the composition is slightly different with higher concentration of non-clay minerals and smaller proportions of smectite and illite.

Although smectite and illite variations are the most obvious, kaolinite and chlorite

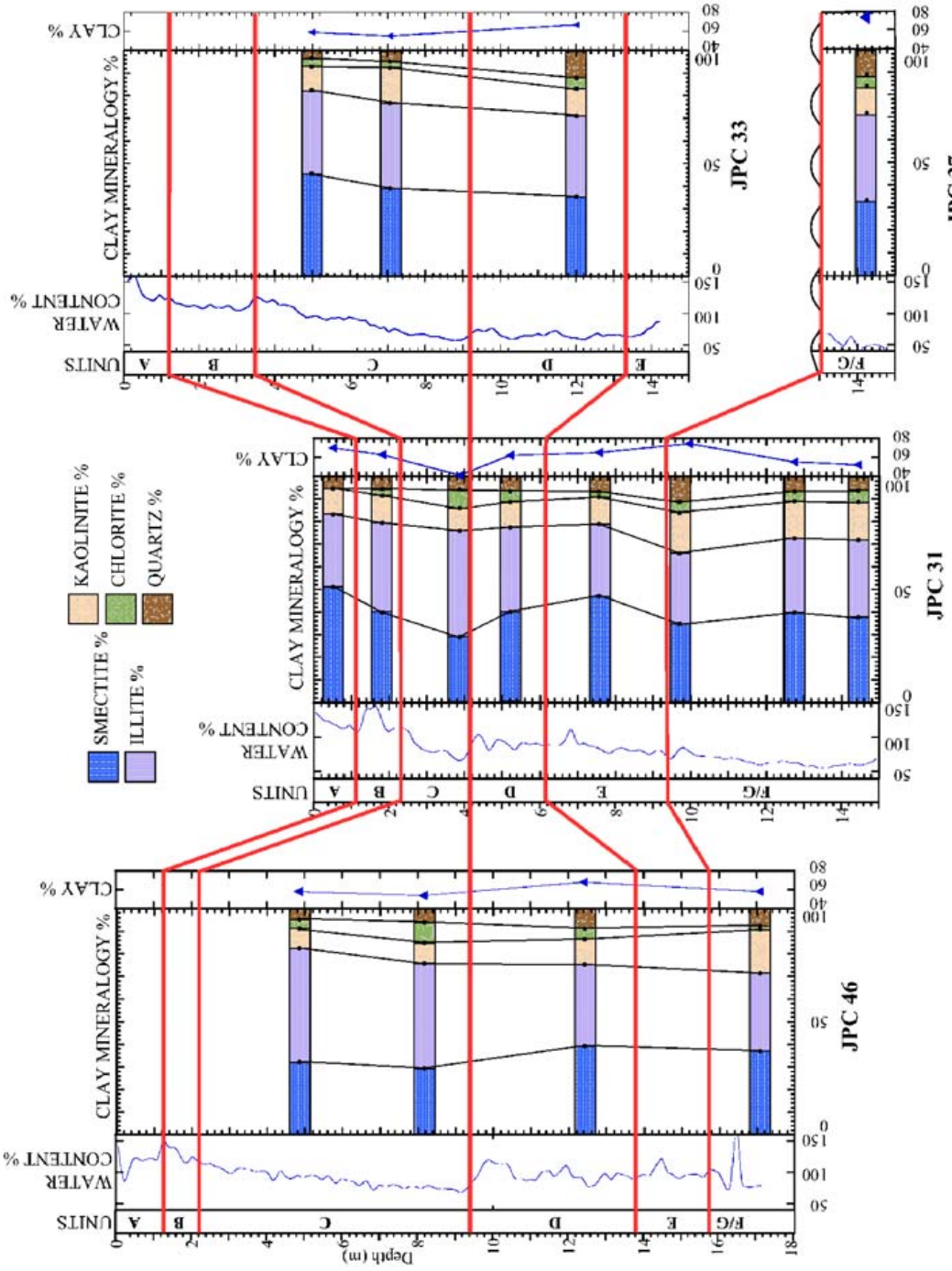

Fig. 15. Clay mineralogy trends. Variations in clay mineralogy with depth and units are shown for cores JPC 46 (upper-slope), JPC 31 (mid-slope), JPC 37 (mid-slope) and JPC 33 (lower-slope).

vary as well. Kaolinite tends to follow the trend of smectite, while chlorite is inversely correlated to it. Quartz and feldspars are present in small amounts, however their concentration is higher in samples of Unit D, Unit B and the red layers at the top of Unit F/G. In addition, changes of the clay mineralogy also correspond to changes in clay content and coarse grain mineralogy, specifically the proportions of biogenic calcite respect to terrigenous minerals (See "Bulk samples and silt fraction" on page 33). Therefore samples with higher smectite content generally contain a larger clay fraction as well as more biogenic calcite rather than terrigenous minerals and vice versa.

The trend described above was based on core JPC 31, located in the mid-slope that was sampled at the greatest resolution. Nonetheless, results from the other cores confirm this trend thereby indicating that the clay mineralogy of each sedimentological unit is spatially homogeneous in the Bryant Canyon area. In Fig. 15 sedimentological units are traced between cores to allow comparing their composition at different locations. It can be noticed that the clay mineral composition of Unit C is approximately the same between core JPC 46 (upper slope) and core JPC 31 (mid slope) but changes toward significantly higher smectite content in core JPC 33 (lower slope). However, the composition of Unit D remains the same in the same three cores. Likewise, Unit F/G maintains similar characteristics in cores JPC 31, JPC 46 and JPC 37.

The dramatic change in composition of Unit C in the lower slope (JPC 33) may derive either from a change in source of sediment or from differential settling of minerals due to current transport. Independent evidence such as thickening of the unit and change in sedimentary structures (Tripsanas, 2000), supports the hypothesis of a different prove-

nance of sediment. Tripsanas (2000) discusses in detail such hypothesis and concludes that Unit C in the lower slope (JPC 33) is composed of sediment resuspended and transported from the GOM basin by bottom currents. While the spatial homogeneity of clay mineralogy may appear counterintuitive, it is consistent with the similarity in the trends of physical properties and magnetic susceptibility across the slope as well as their changes in correspondence of the major unit boundaries.

The sedimentological units so far used as reference closely relate to oxygen isotope stages and correspondent glacial-interglacial cycles, hence so does the mineralogy. To better characterize the relation between mineralogy and glacial-interglacial cycles it is useful to categorize the mineral results. Three mineral facies were subdivided based on the mineralogy results (Fig. 16), with the aid of a cluster analysis, performed using smectite and illite fractions as discriminant variables.

1) Clay fraction rich in smectite (~48%), with lesser amounts of illite (~30%), relatively abundant in kaolinite (~11%) and poor in chlorite (~2%). The calcite to quartz XRD peak intensity ratio indicates that biogenic carbonate is more abundant than quartz. This facies is represented by sediments from oxygen isotope stages 1 and 5 (Unit A and Unit E) that correspond to the present and last interglacial maxima (Fig. 16).

2) Clay fraction rich in illite (~48%), with lesser amount of smectite (~30%), relatively abundant chlorite (~7%) and less kaolinite (~9%). Among the non-clay, quartz is very abundant, while calcite and dolomite are present just in small and about equal proportions. This facies characterizes deposits of the last glacial maximum (Unit C), correspond-

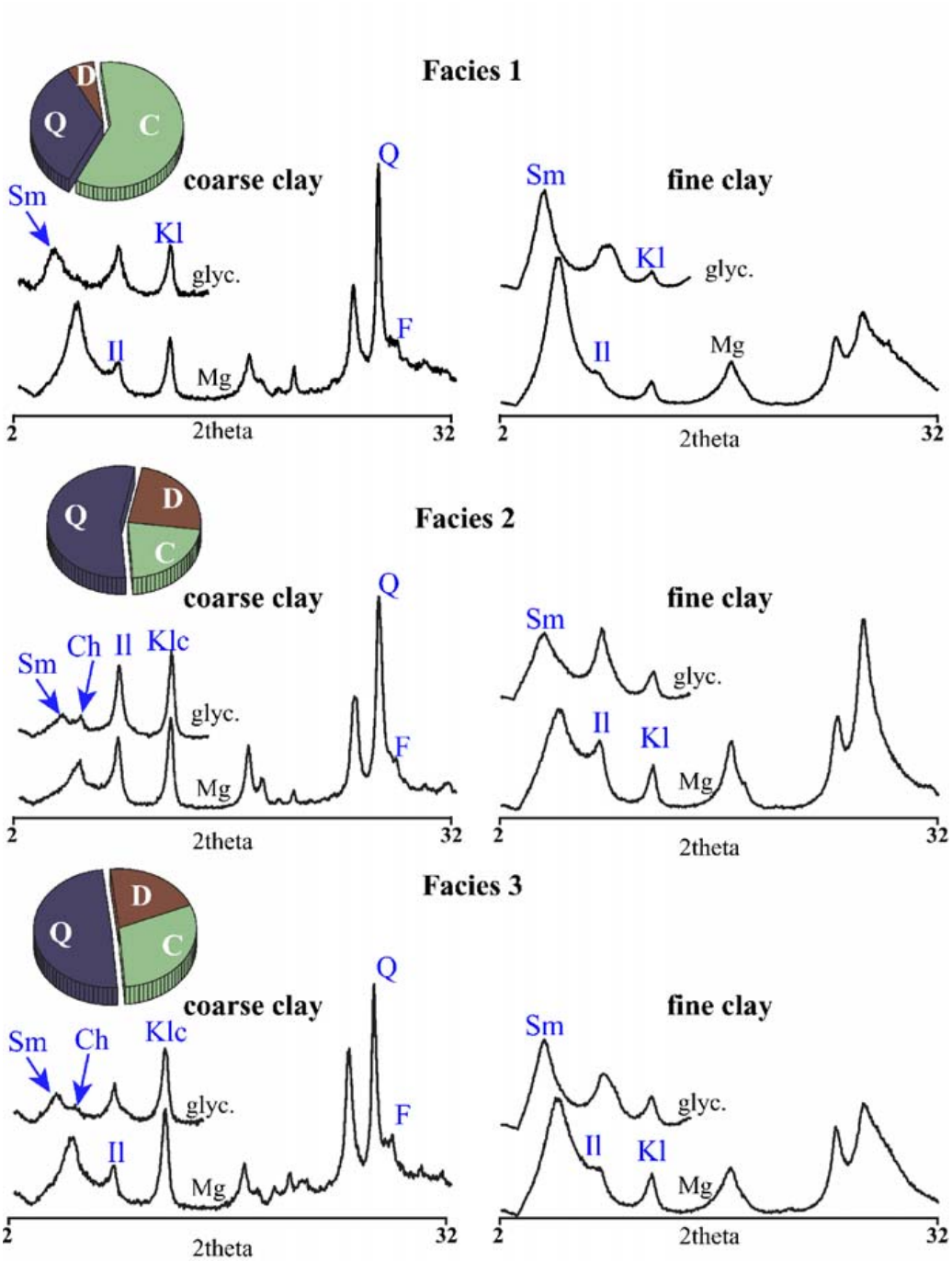

Fig. 16. Typical XRD patterns of the main associations identified. The XRD shown refer to the Mg saturation (Mg) and glycerol solvation treatments (glyc.) of the coarse (left) and fine (right) clay fractions. The following samples are used to represent each facies: 31-1 (facies 1), 46-2 (facies 2) and 31-6 (facies 3). The basal peak of minerals are indicated in the figure: sm: smectite, Ch: chlorite, Il: illite, Klc: kaolinite and chlorite, Kl: kaolinite, Q: quartz, F: feldspars. The pie charts on top illustrate the average intensity ratio of quartz (Q), calcite (C) and dolomite (D) in the bulk sample XRDs. These ratios are only estimates of relative proportions of these minerals and do not measure absolute abundances.

ing to the oxygen isotope stage 2 (Fig. 16).

3) Clay mineralogy characterized by similar proportion of smectite (~38%) and illite (~34%) and high kaolinite content (~14%). Little chlorite is present (~4%), but quartz and feldspars are rather abundant in the clay. Quartz is also very abundant in the non-clay fraction, where it largely exceeds calcite and dolomite. Sediments from stages 3,4 and 6 fall into this category (Fig. 16).

Overall, the mineral facies strongly indicate that significant environmental changes occurred in the Bryant Canyon area in response to climate and eustatic sea-level changes. The characteristics of Facies 1 are consistent with the depositional regime of interglacial maxima, with abundant smectite, high clay content but also more forams. In fact in interglacial maxima river tend to discharge on the continental shelves and only the finest fraction of river suspended sediment reaches the slope. Furthermore, source rocks on land are subjected to intense chemical alteration therefore yielding a larger proportion of secondary minerals like smectite and kaolinite. The limited terrigenous input also explains the larger concentration of biogenic carbonate (from foram shells) of Facies 1.

Facies 2 records the deposition of the last glacial maximum (stage 2) during which vast portions of the Mississippi River drainage basins, part of which are sources of smectite, were covered by the Laurentide ice sheet. Furthermore, mechanical weathering of source rocks is more intense than chemical thereby favoring formation of illite and chlorite rather than smectite or kaolinite. As a consequence, smectite is scarce while illite is very abundant in the sediments of Facies 2. In addition, during stage 2 the terrigenous input is larger as rivers discharge their load directly to the continental slope. Correspondingly,

Facies 2 is characterized by only a small fraction of biogenic carbonate and by a larger grain size. A similar increase in illite in sediments from stage 2, contrasting with high smectite content of sediments from stage 1, was also found in sediments from Orca Basin (Brown and Kennett, 1998), Pigmy Basin (Bouma et al., 1986) and even in sediments of the Carolina slope (Çagatay et al., 2002). Such a consistency strongly supports that changes in rock alteration products occurred and addresses the usefulness of clay mineralogy as paleoclimate proxy.

The effect of clay mineralogy on physical properties

Atterberg limits

In the following paragraphs an attempt will be made to identify those compositional factors that most affect the physical properties of the GOM continental slope sediments. Atterberg limits were extensively used in these correlations as they depend on the same factors that all sediment geotechnical properties depend on (Terzaghi cited by Mitchell, 1993), for their independence on depth and for the large availability of correlations with other geotechnical properties.

The clay mineral abundances used for correlations are referred to the whole sample, unless otherwise specified, according to Equation 4 :

$$M = M_C \bullet C \qquad 4)$$

Where: M = mineral fraction (%) and C = clay fraction (%) and M_C is determined from Equation 3

Plots of Atterberg limits versus clay and smectite content are illustrated in Fig. 17.

Clearly, higher clay content and smectite content cause the Atterberg limits to increase, however the effect of smectite content is more significant than that of clay content. The greater importance of smectite is not only evident from the data distribution on the plots but also from significantly higher correlation coefficients (Table 4). In fact, the total variance explained (coincident with r^2, for a linear fit) by clay content is only 59% as opposed to 75% explained by smectite.

Compared to other studies (e.g. Al-Shayea, 2000; Skempton, 1970) the correlation coefficient between Atterberg limits and clays herein reported is low. The apparent contradiction simply derives from differences in procedures and materials used. Studies that yield very high correlation coefficients (higher than 0.8) between clay content and Atterberg limits are conducted by mixing the same clay with different proportions of silt or sand. Therefore, they do not test the role of clay minerals. Differently, studies conducted on natural samples yield correlations comparable to those herein reported (Ohtsubo et al., 2002; Sridharan, 1986; Borchardt, 1977). Undoubtedly, abundant smectite corresponds to abundant clay as well, since this mineral cannot grow larger than clay size; however the opposite is not necessarily true, as clays can comprise many minerals. In this study a significant correlation was indeed found between clay content and smectite content ($r = 0.75$) nonetheless, the dominance of smectite clearly emerged from the coefficient of correlations.

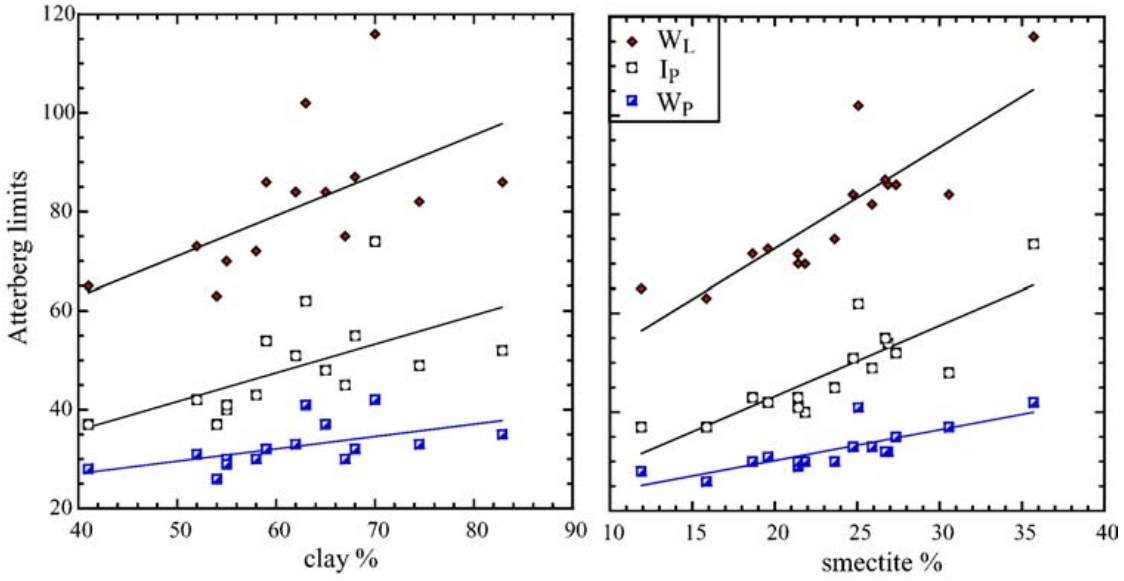

Fig. 17. Correlation of Atterberg limits with clay and smectite content. Smectite abundance is relative to the whole sample.

Table 4

Correlation between clay minerals, clay content and Atterberg limits

	smectite	illite	kaolinite	chlorite	quartz	clay
W_L	0.86**	0.32	0.1	-0.25	0.39	0.77
W_P	0.86**	0.19	0.24	-0.3	0.45	0.75
I_P	0.84**	0.4	0.1	-0.25	0.39	0.8

The effect of the other minerals composing the clay fraction on Atterberg limits was examined as well, by regression analysis (Table 4). None of them yield a statistically significant correlation with Atterberg limits, although general trends can be recognized in the plots (Fig. 18). Most likely, these trends are a consequence of the interrelations

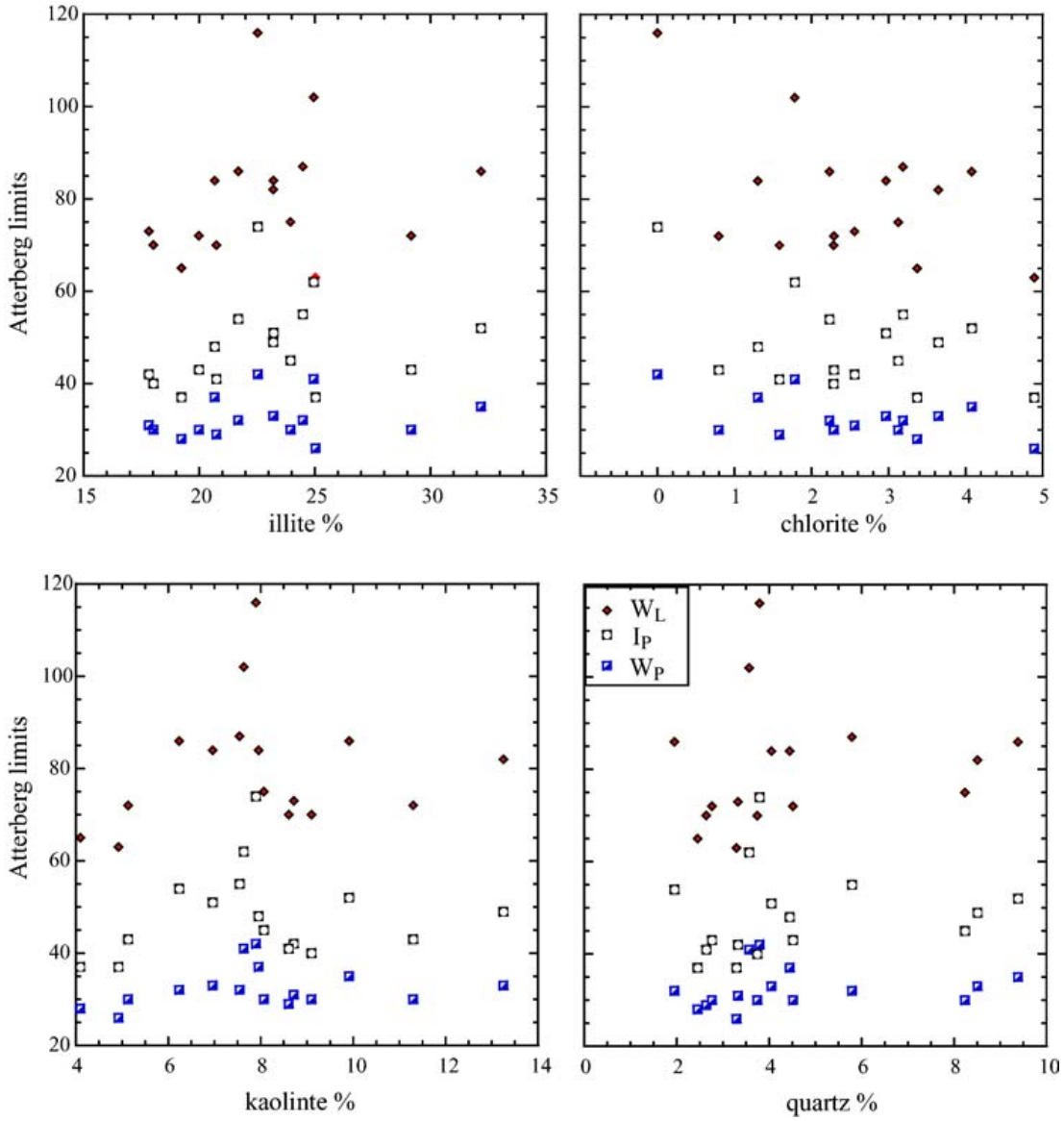

Fig. 18. Clay mineral abundances and Atterberg limits. Mineral abundances are relative to the whole sample.

between clay minerals that were discussed in the previous paragraphs (See "Clay mineral abundances and their variations" on page 43).

Overall, these results indicate that when smectite is present in the clay fraction its

influence on physical properties prevails on that of other components. Furthermore, it is important to notice that even small amounts of smectite make a significant difference in physical properties. In fact these samples contain at most 38% of smectite respect to total weight, nonetheless their physical properties are dominated by this mineral.

An additional observation emerges from the relations just discussed. Each of the Atterberg limits yields similar correlations with the same compositional factors, in other words they are affected in a similar way by clay mineralogy and clay content. However, the W_L yields better correlation coefficients than W_P or I_P. This is most likely caused by higher subjectivity in determining the W_P rather than W_L. Furthermore, Burland (1990) based on a statistical study, concluded that small errors in W_L and W_P become significant when one is subtracted from the other, especially at low I_P values. Similarly, Pandian and Nagaraj (1990) concluded that the W_L can alone predict engineering behavior of sediment.

Fractionation of coarse (2-0.2 μm) and fine (<0.2 μm) clay makes it possible to compare the effect of both on Atterberg limits (Fig. 19). Interestingly, Atterberg limits correlate with smectite content in the fine clay just as well as with total smectite fraction. Differently, the correlation with coarse clay smectite is relatively poor. Such results in addition to reflecting the small size of smectite, manifest the profound relevance of colloidal properties, such as large surface area and surface reactivity, on physical properties. In fact, it is because of smectite surface properties that this mineral can retain as much as twice its weight in water, with obvious consequences on W_L. As a consequence, it is probable that other clay minerals with surface properties similar to those of smectite (e.g. ver-

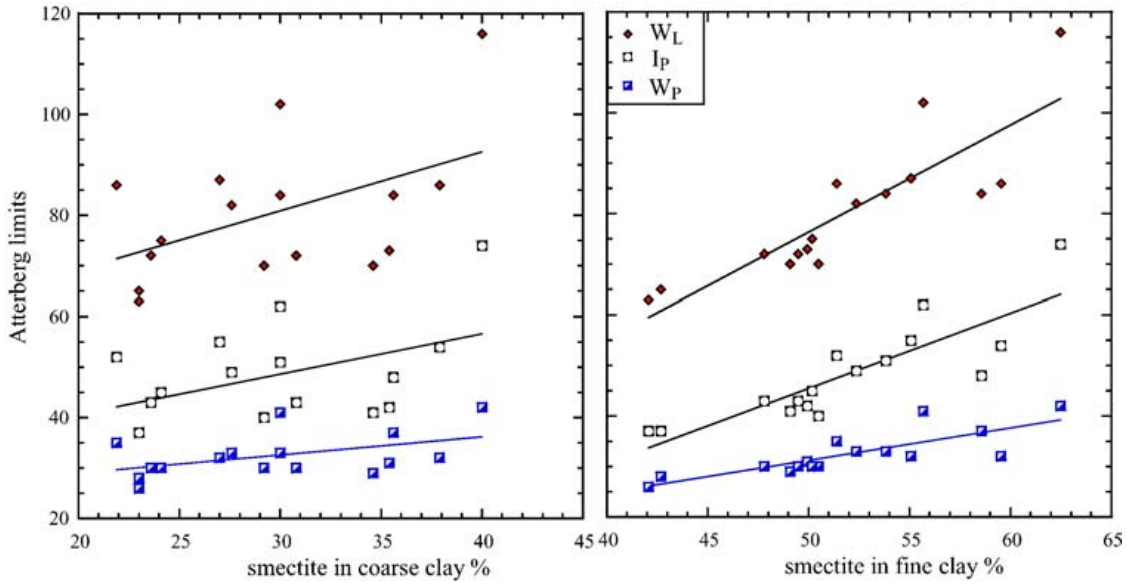

Fig. 19. Atterberg limits and smectite content in the coarse and fine clay fractions.

miculite) yield similar effects as well. Although this hypothesis cannot be tested on the basis of the samples available for this study, it addresses a possible limitation to the applicability of these results.

After establishing the dominant role of smectite on cohesive properties, it is important to verify the influence of other soil components and compare this model with others found in the literature. It was pointed out initially (page 2) that generally applicable models based on artificial mixtures do not reliably predict the clay mineralogy of natural sediments. Nonetheless, general models represent a valuable term of comparison.

In Fig. 20 the smectite vs. liquid limit model derived in this study is compared to models by Mitchell (1993) and Grabowska-Olszewska (2003). The two models by Mitchell (1993) are based one on a theoretical linear relationship between smectite and liquid

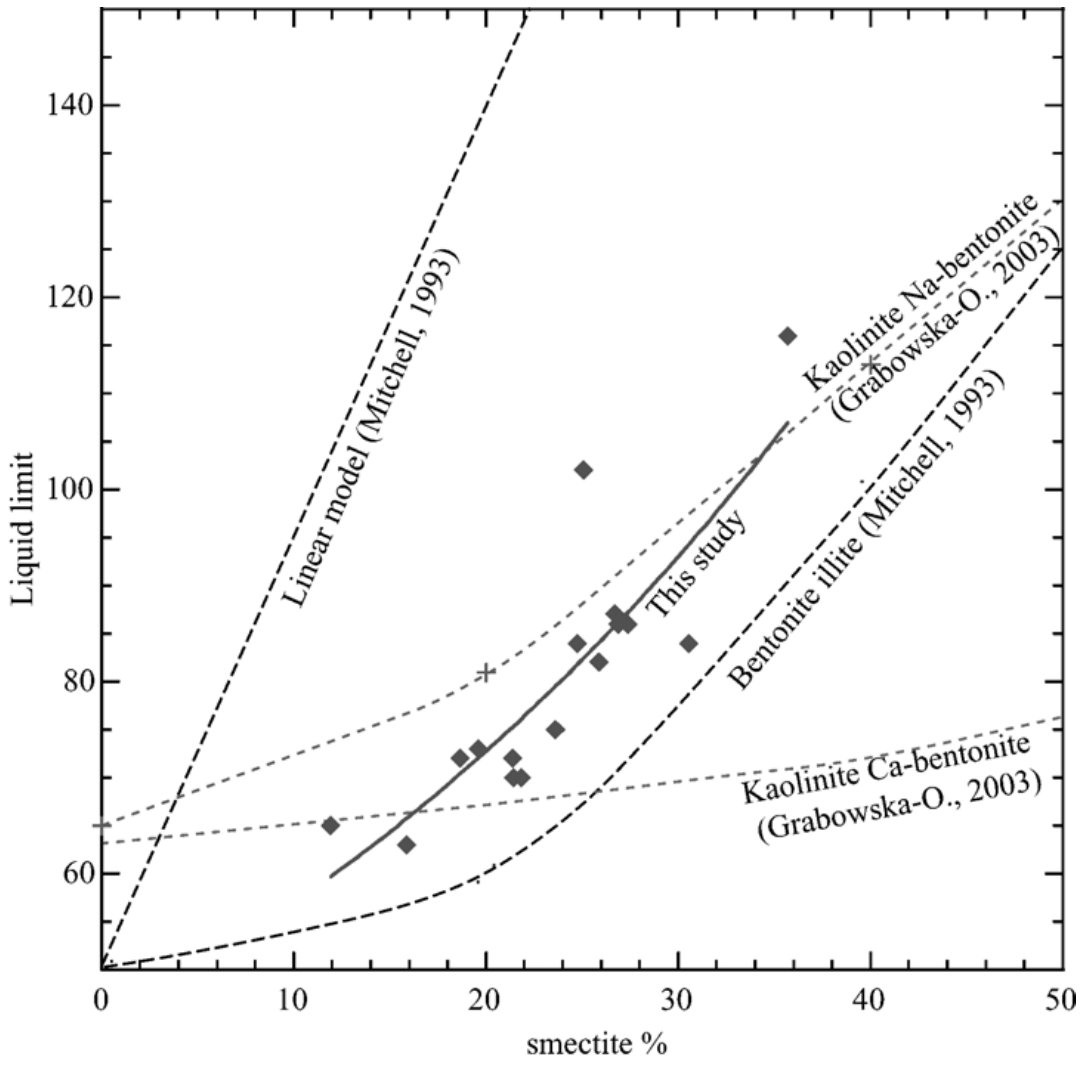

Fig. 20. Comparison with other models. The W_L-smectite correlation obtained in this study is compared with a theoretical linear model and a illite-smectite mixture model by Mitchell (1993) as well as with models of kaolinite and smectite mixtures by Grabowska-Olszewska (2003).

limit, obtained linking the liquid limit of a pure illite with that of a pure Na-smectite; the other model is based on mixtures of different proportions of illite and smectite. The trend described by illite-smectite mixtures shows that interactions between the two minerals are

not linear. It appears that smectite begins to have a significant effect on the liquid limit only when its weight fraction is higher than ~20%. On the other hand, the two models by Grabowska-Olszewska (2003) are based on mixtures of kaolinite with Na-saturated and Ca-saturated smectite thus highlighting the different behavior of smectite depending on chemical environment. The slight difference (2.5) in liquid limit of the two initial samples of pure kaolinite are the results of small errors in the determination. The two plots indicate that Ca-saturated smectite has a small influence on the liquid limit. Conversely, addition of Na-smectite significantly affects the liquid limit.

The data from this study describe a trend that is parallel to that of illite-smectite mixtures of Mitchell (1993) although offset toward higher values of liquid limit for a given smectite content. This similarity is consistent with the observation that illite is indeed the other dominant clay mineral in the samples. Accordingly, the offset with respect to Mitchell's trend may be a consequence of the presence of silt and/or of a different chemistry of pore water. Overall, the differences between this and other models demonstrate the extreme variability in the interactions between clay minerals with each other and their environment that also correspond to different effect on physical properties. As a consequence, models based on a more focused approach can yield more reliable information than general ones.

It should be noticed that in the previous paragraphs a linear correlation was used for the smectite-W_L relationship that yield the following relationship:

$$W_L = 33 + 2.05SM, \quad r^2 = 0.72 \qquad 5)$$

Equation 5 predicts a liquid limit of 33 if smectite is not present in the clay fraction. Nev-

ertheless since samples with no smectite or of pure smectite were not available, this relation is only applicable for smectite contents between ~ 10 and ~ 40 %. Based on the correlation coefficient and variance the linear fit appears sufficiently representative; however, the comparison with Mitchell's model suggests that the relationship is not linear. An exponential fit actually yields a better correlation, and a W_L correspondent to 0% smectite more similar to that reported for illitic sediment (Mitchell, 1993):

$$W_L = 44.5SM^{0.025} \quad r^2=0.75 \qquad 6)$$

This latter model is shown in Fig. 20. Similarly to the linear model, the model described by Equation 6 is applicable for a range of smectite weight fractions between 10 and 40 %.

Other studies in the literature also address the relationship between CEC and Atterberg limits (Christidis, 1998; Thomas et al., 2000; Sridharan, 1982; Sridharan, 1986; Bennett et al., 1981). In this study the high degree of interdependence between smectite content and CEC does not allow separating the effect from one another; not surprisingly, the correlation of W_L with CEC is just as good as that with smectite. If other minerals bearing an unsatisfied layer charge were present (e.g. vermiculite, halloysite) or even different types of smectite, the results could differ. In fact, depending on the distribution (tetrahedral or octahedral) and magnitude of partially unsatisfied structural charge, measured by the CEC, mineral surface chemical properties can vary enormously (Dixon and Weed, 1989; Bennett et al., 1981). Nonetheless, CEC can be determined with a high degree of accuracy and precision, in contrast with a more subjective and interpretative quantification of smectite. Thus it is a good choice as term of comparison between samples from different regions and even more so when the clay mineralogy (hence minerals contributing to the CEC) is

known. Because of its relation with clay mineralogy and their properties, the CEC in combination with W_L is used as indicator of soil swelling behavior (Thomas et al., 2000).

In order to characterize and classify soils, Atterberg limits are plotted on the Casagrande, or Plasticity Chart (Fig. 21). The data from this study fall just above the A-line and follow a similar trend. A best fit through the data yields the following equation:

$$I_P = 0.7(W_L - 11.8),\ r^2 = 0.98 \qquad 7)$$

Based on the Unified Soil Classification System (USCS) the sediments can be classified as inorganic clays of high to extremely high plasticity (CH). It has become common use to deduce the clay mineralogy based on the location of data on the Plasticity chart, with respect to the A-line and the U-line. Smectitic soils are expected to plot just below the U-line, whereas illitic soils just above the A-line (See "Literature review" on page 8). Accordingly, all samples from this study would be categorized as illitic. Even just considering the extreme range of variation in smectite composition, the subdivision appears unlikely. Certainly the data from this study disprove such model. The variation in smectite and illite content in these samples was extensively explained throughout the manuscript, and a well supported argument was presented for the dependence of liquid limit on smectite content (See page 57).

Moreover, as also highlighted in Fig. 21, the smectite trend in these data increases in concurrence with W_L and I_P, and is approximately parallel to the A-line. In contrast, variations in illite content do not follow any specific trend with W_L and I_P (Table 4). It is possible that shifting toward the U-line depends on the type of cations saturating clay min-

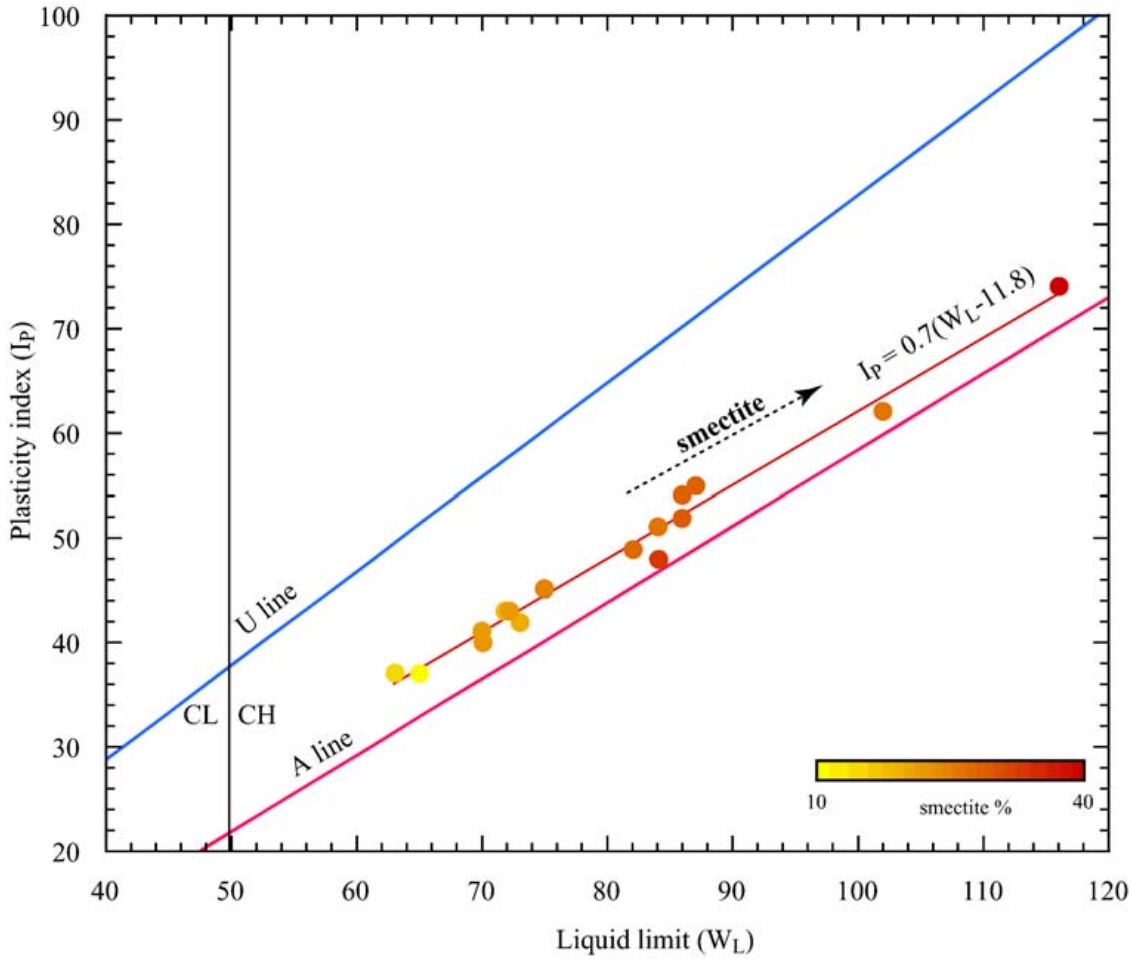

Fig. 21. Plasticity chart. A color scale is used to indicate the smectite content of the samples. Note the increasing smectite with increasing W_L and I_P.

erals and smectite particularly. Actually, the position of the U-line was first determined based on Na-montmorillonite that is one of the most swelling types of smectite because of the properties of the monovalent cation filling the interlayer. However, smectite does not reach similar degree of water retention and swelling capacity when saturated with a mixture of different cations, as is most commonly the case in nature. Specifically, in marine

sediments the composition of the mixture of cations that saturate smectite is a function of sea water composition and of cation affinity to smectite. Nonetheless, the effect of smectite on the engineering properties of sediments is significant.

Bulk density and derived variables

The relations so far discussed concerned properties that are measured on remolded samples therefore are not directly affected by depth. In contrast, physical properties like bulk density, water content, P-wave velocity and shear strength change during the burial history of sediments. Consequently, correlations of these properties with clay content and mineralogy are only meaningful if performed on sediments with same stress history. This is not the case for the samples used in this study hence it is not surprising that a linear regression analysis does not yield significant correlations. However, all physical property profiles present well discernible variations in rate of change as well as spikes of high or low values in relationship to lithology and compositional changes.

Skempton (1970) argued that a linear relation exists between void ratio (e_0) and the log of effective overburden pressure (P_0) for the same type of clay, hence the void ratio of a clay at a certain pressure P_0 only depends on the type of clay. Accordingly, changes in slopes and offsets in a e_0-P_0 plot should reflect changes in composition (Skempton, 1970; Burland, 1990). Fig. 22 shows the e_0-P_0 plot of JPC 31. The overburden pressure was calculated by integrating bulk density over depth according to Equation 2 on a logarithmic scale. The corresponding depth is also shown for reference. The void ratio trend is compared to the smectite and clay content from JPC 31 samples, since these are the two com-

positional factors that were proven to affect physical properties. From Fig. 22 it can be noticed that the general trend of decreasing void ratio with increasing overburden pressure and depth is interrupted by considerable offsets in correspondence of changes in clay and smectite content.

Burland (1990) implementing the work of Skempton (1970), deduced a relation between the intrinsic void ratio at 100 kPa of overburden pressure (e_{100}*) and the void ratio at the liquid limit (e_L). The term 'intrinsic' refers to the properties of reconstituted clays (Burland, 1990) that only depend on their composition. It will be shown later how environment and modes of deposition also influence physical properties. Not surprisingly, e_{100}* increases exponentially with smectite content, yielding a curve fit resembling that W_L and an excellent correlation coefficient (r = 0.86). Therefore, it can be concluded that the W_L of clays also represents changes in the W_C and void ratio profile related to changes in clay mineralogy.

The relationships so far established can be related to the forces that control the Atterberg limits and the cohesive properties of clays. The two mechanisms discussed in the literature point one to the net interparticle attractive forces and the other to the viscosity of the double layer (and interlayer) water (Sridharan, 1988). The correlation of grain size with Atterberg limits supports the influence of net attractive forces, as these are a function of specific surface area (hence grain size). On the other hand, the larger influence of smectite on Atterberg limits suggests a correspondent larger effect of the double-layer water. In fact, according to Mitchell (1993) the increase in W_L with increasing smectite is related to

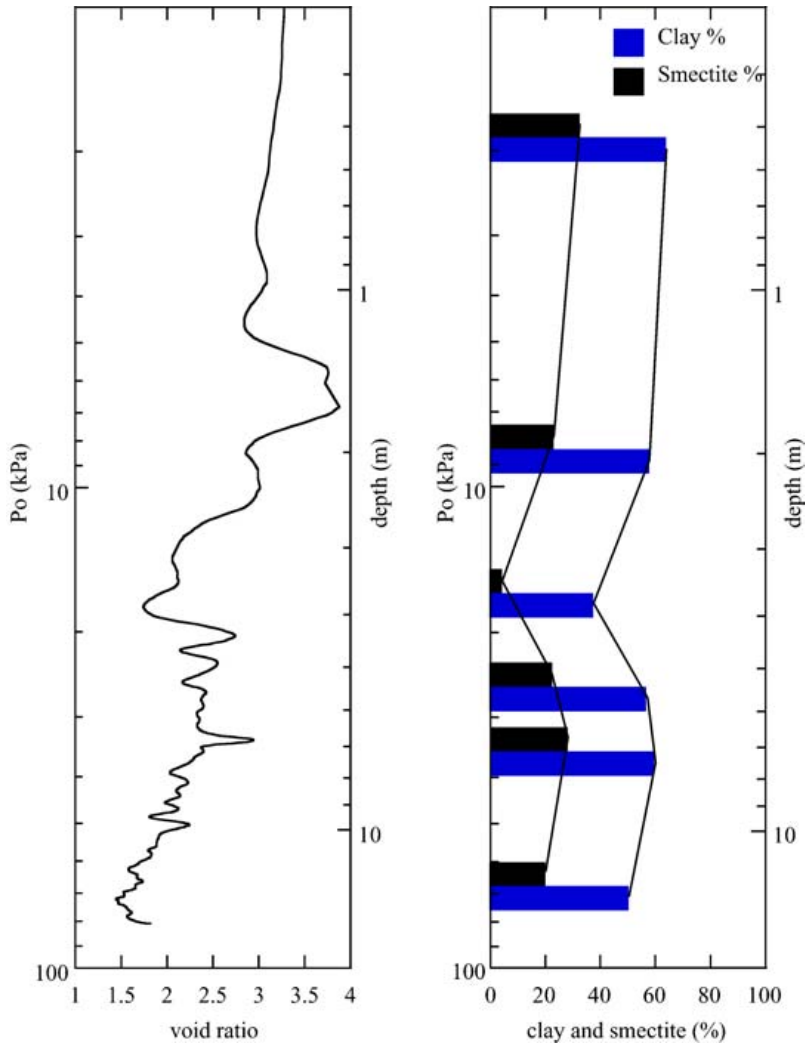

Fig. 22. Void ratio depth-pressure profile compared with clay and smectite content. Vertical pressure (Po) was calculated by integrating bulk density over depth (Equation 2). A log scale was used for vertical pressure and depth. The plots shown refer to core JPC 31. Note the large void ratio offsets in relationship to changes in smectite content.

the interlayer water which is a good portion of double-layer water. This relation would also explain the greater effect of pore water chemistry on the properties of smectitic soils (Sridharan, 1988; Mathew, 1997). Based on the same concept, Brown and Ransom (1996) demonstrated the significant effect of smectite inter-layer water on the porosity of sediments.

Shear strength and the influence of rates of deposition

In spite of the normal consolidated (NC) state of the sediment, the depth profile of shear strength abruptly changes in correspondence of the boundary between Unit C and Unit D (Fig. 6). The small depth gradient and little variability of the top three units is substituted by a larger gradient and greater variability throughout the units below. The difference between the gradient of the upper and lower interval is larger where Unit C is thicker.

The boundary between units C and D corresponds to a considerable change in mineralogy and depositional rates, both factors that may affect the shear strength. The availability of oxygen isotope curves from core JPC 31 (Elston and Slowey, personal communication) offered the opportunity to investigate the effect of sedimentation rates. Fig. 23 illustrates the age model for JPC 31. The model is based on the dates of stratigraphic markers that can be easily correlated among the other cores, for which direct dating is not available.

Successively, S_U gradients were calculated relative to the same depth intervals used for sedimentation rates, thus allowing their comparison. Because direct dating determinations were only available from one core, and for the limits in the accuracy of vane shear measurements, these data should only be considered as gross estimates.

Despite these limitations, Fig. 24 shows that a correlation between sedimentation rates (in logarithmic scale) and S_U gradient exists, demonstrating the importance of the depositional regime on physical properties. In the right plot of Fig. 24 the S_U gradient is

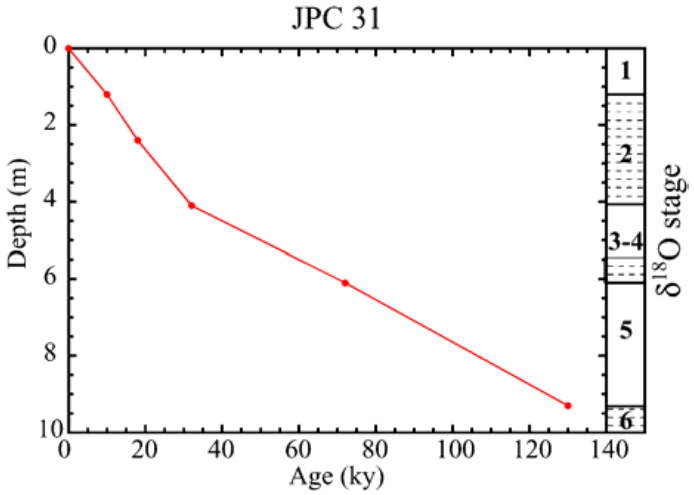

Fig. 23. Age model of core JPC 31. Sedimentation rates were determined from the slope of the lines connecting data. Note that changes in slope correspond to changes in sedimentation rates.

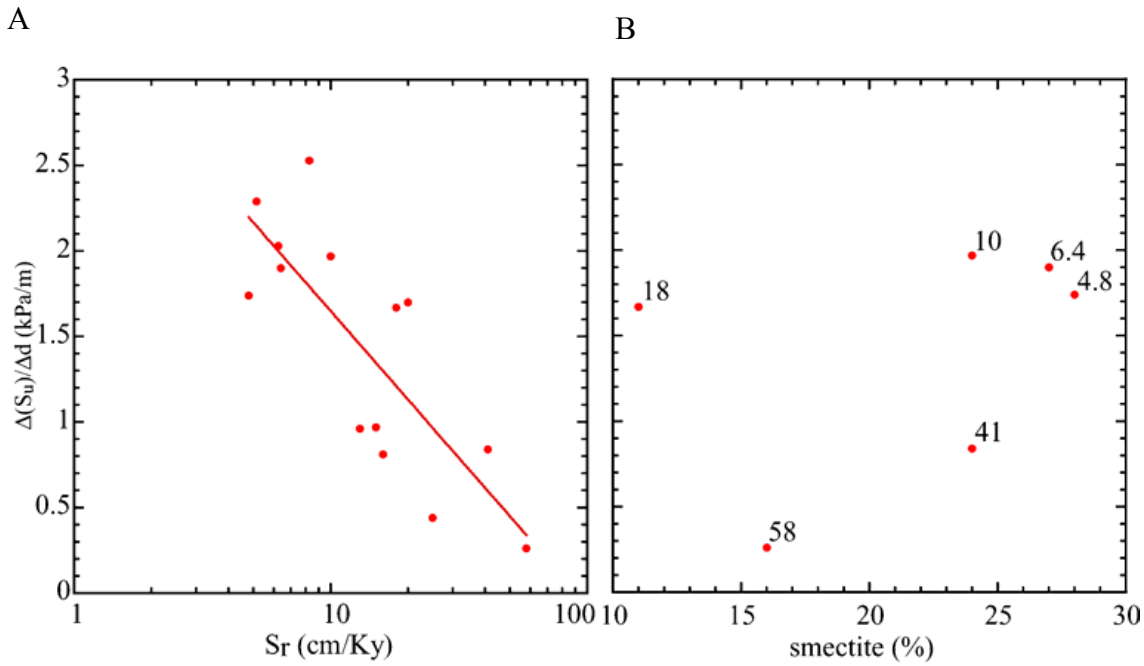

Fig. 24. Sedimentation rates and shear strength. (A) Correlation between sedimentation rates (Sr) and shear strength depth gradient ($\Delta S_U/\Delta d$). A linear regression yielded the following equation: $\Delta S_U/\Delta d = 3.37 - 1.72\log(Sr)$. (B) Smectite content in relation to $\Delta S_U/\Delta d$ and sedimentation rates (indicated by the numbers next to data points).

instead compared to smectite content, the mineral having the most influence on physical properties (See “Atterberg limits” on page 52); sedimentation rates are indicated by the numbers next to the points. The data distribution on the plot, on one side reflects the higher smectite content of slowly deposited sediments which causes the clustering in the top right corner of the plot; on the other side, it shows a lack of correlation between the two variables. The relevant role of modes and rates of deposition on physical properties has been recognized by several other studies, and attributed to microfabric (e.g. Mitchell, 1993; Bennett et al., 1981; Burland, 1990; Skempton, 1970). The micro-fabric acquired by the sediment at the time of deposition profoundly influences physical properties and their progression with depth (Mitchell, 1993; Bennett, 1999; Burland, 1990).

SUMMARY AND CONCLUSIONS

1) This study assessed the clay mineralogy of Bryant Canyon sediments, deposited during the last 6 oxygen isotope stages, as well as its spatial and depth variability. It was determined that smectite and illite are the dominant clay minerals, their sum making up 75-80% of the clay size fraction of the sediment. Kaolinite and chlorite compose the remaining of the clay, although traces of non clay minerals (quartz and feldspars) are present as well. The main minerals composing the silt and sand size fractions are instead quartz, calcite, dolomite and feldspars.

2) Three different mineral facies were recognized that alternated with depth in concurrence with changes in climate, distance from the source and of the extent of the Mississippi drainage basin itself. The main differences between these associations reside in the relative abundance of smectite and illite in the clay fraction as well as the amount of biogenic carbonate in the non-clay fraction. During interglacial high stands, less input of terrigenous sediments, more intense chemical alteration of parent rocks accompanied by higher productivity yielded a facies rich in smectite and biogenic carbonate, in concomitance with interglacial periods. In contrast, more terrigenous input, dominance of mechanical weathering on land and the obstruction of portions of the Mississippi Basin by the Laurentide ice sheet yielded an illitic facies, with lesser amounts of pelagic carbonates. In the remaining facies, deposited during other glacial or transitional periods the effect of large terrigenous input is reflected in a relatively high amount of clay size quartz and feld-

spars. However, smectite is rather abundant, in concentration similar to that of illite and biogenic carbonate is abundant as well.

3) Although diagenetic transformations of minerals cannot be excluded and are, to some extent, probable, their influence on the clay mineral association is minimal, if not negligible. Furthermore, any mineral transformation induced by the chemistry of sea water appears to have ceased soon after deposition. In fact, based on XRD peak characteristics and NEWMOD© simulation it was concluded that the same minerals, although in different proportions compose all the samples.

4) The clay mineralogy of the sedimentological units does not vary significantly across the slope; in other words a specific mineral/clay mineral association marks each of the units. In this respect, the character of clay mineralogy is consistent with that of physical property profiles as described by Bryant et al. (2000). Certainly a connection between clay mineralogy, as well as clay content with the characteristics of the physical property profiles is not surprising and was actually illustrated by this study. An implication of the homogeneous character of the sedimentological units, is the possibility to infer the clay mineral character of sediments from the Bryant Canyon simply based on MSCL profiles. Furthermore, similar clay mineralogy trends respect to glacial cycles were found in Pigmy Basin, Orca Basin and the Carolina continental slope.

5) The most significant conclusion of this study is the relationships established between sediment composition and physical properties. It was demonstrated that smectite directly affects Atterberg limits, and to a larger extent than clay content does. Other minerals may attenuate or exacerbate the influence of smectite but they have no direct effect

on physical properties. More importantly, an equation was derived to describe such relation and compared with models found in the literature. The better understanding that derives from such comparison may prove useful in formulating better models to describe the mechanical behavior of the Gulf of Mexico continental slope sediments. A linear fit approximately parallel to the A-line described the data distribution in the Plasticity chart. Samples higher in smectite plotted in correspondence of higher values of liquid limit and plastic limit, independently of clay content or of other mineral abundance.

6) It was demonstrated that the liquid limit can alone represent the composition of sediments, at least in the case of samples from the same depositional environment. The other Atterberg limits, as well as indexes although useful for classification purposes are less indicative of composition. It was also shown that the liquid limit can be used to represent variation in the magnitude of water content (as well as related variables) with depth related to changes in composition and particularly smectite content.

7) Finally, the influence of depositional regimes on physical properties was discussed. A comparison between undrained shear strength and sedimentation rates was used to investigate such effect. It was shown that changes in the rate of increase of undrained shear strength with depth correlate with the rate of deposition.

In essence, this thesis assessed the enormous importance of smectite on the physical properties of marine sediments, based on analyses performed on natural sediments. Relationships were determined between physical properties and clay mineralogy for sediments of the northwestern GOM continental slope. Furthermore, it established a link between clay mineralogy and oxygen isotope stages that offers a strong basis for compar-

ison with studies that may be conducted in the future in different locations.

REFERENCES

Abdullah, W.S., Alshibli, K.A., Al-Zou'bi, M.S., 1999. Influence of pore water chemistry on the swelling behavior of compacted clays. Applied Clay Science, 15: 447-462.

Acemana, S., Lahav, N., Yariv, S., 1999. A thermo-FTIR-spectroscopy analysis of Al-pillared smectites differing in source of charge, in KBr disks. Thermochimica Acta, 340-341: 349-366.

Alexiades, C.A., Jackson, M.L., 1966. Quantitative clay mineralogical analysis of soils and sediments. Clays and Clay Minerals, 14: 35-52.

Al-Shayea, N.A., 2000. The combined effect of clay and moisture content on the behavior of remolded unsaturated soils. Engineering Geology, 62: 319-342.

Aoki, S., Kohyama, N., 1991. The vertical change in clay mineral composition and chemical characteristics of smectite in sediment cores from the southern part of the Central Pacific Basin. Marine Geology, 98: 41-49.

ASTM-D4648-94, 1994. Laboratory miniature vane shear test for saturated fine-grained clayey soils, Annual Book of ASTM Standards, Philadelphia, PA.

ASTM-D4318-98, 1998. Standard test method for liquid limit, plastic limit, and plasticity index of soils, Annual Book of ASTM Standards, Philadelphia, PA.

ASTM-D2487-00, 2000. Standard classification of soils for engineering purposes (Unified Soil Classification System), Annual Book of ASTM Standards, Philadelphia, PA.

Bean, D.A., 2000. Correlation between physical and acoustic properties in surficial sediments of the northwest Gulf of Mexico, M.S. Thesis, Texas A&M University, College Station, TX, 95 pp.

Bennett, R.H., Bryant, W.R., Keller, G.H., 1981. Clay fabric of selected submarine sediments: fundamental properties and models. Journal of Sedimentary Petrology, 51(1): 217-232.

Bennett, R.H., R.H., Ransom, B., Kastner, M., Baerwald, R. J., Hulbert, M. H., Sawyer, W. B., Olsen, H., Lambert, M. W., 1999. Early diagenesis: impact of organic matter on mass physical properties and processes, California continental margin. Marine Geology, 159: 7-34.

Bernas, B., 1968. A new method for decomposition and comprehensive analysis of silicates by atomic absorption spectrometry. Analytical Chemistry, v.39, p.1210-1216

Borchardt, A.G., 1977. Clay mineralogy and slope stability. Special Report 133, California Division of Mines and Geology, Sacramento, CA.

Borchardt, A.G., 1984. Stabilization of landslides: effects of various chemicals on the laboratory shear strength of an expansive soil. Spec. Rep. Calif. Div. Mines Geol., v.155.

Bouma, A.H., 1983. Intraslope basins in the Northwest Gulf of Mexico: a key to ancient submarine canyons and fans. AAPG Spec. Pub., 32: 567-581.

Boyce, R. E., 1976. Definition and laboratory techniques of compressional sound velocity and wet-water content, wet-bulk density, and porosity parameters by gravimetric and gamma ray attenuation techniques. In: Schlanger, S. O., Jackson, E. D., et al. (Eds.), Initial Reports of the Deep Sea Drilling Project. Government Printing Office, Washington, DC, pp.931-951.

Brown, P.A., Kennett, J.P., 1998. Megaflood erosion and meltwater plumbing changes during last North American deglaciation recorded in Gulf of Mexico sediments. Geology, 26(7): 599-602.

Brown, K.M., Ransom, B., 1996. Porosity corrections for smectite-rich sediments: impact on studies of compaction, fluid generation, and tectonic history. Geology, 24(9): 843-846.

Bryant, W.R., Bryant, J.R., Feeley, M.R., Simmons, G.R., 1990. Physiographic and bathymetric characteristics of the continental slope, Northwestern Gulf of Mexico. Geo-Marine Letters, 10: 182-199.

Bryant, W.R., Bean, D.A., Liu, J.Y., Dunlap, W., Silva, A.J., 2000. Geotechnical stratigraphy of continental slope sediments, northwest Gulf of Mexico, In: Proceedings Offshore Technology Conference, Houston, TX, pp.549-558.

Burland, J.B., 1990. On the compressibility and shear strength of natural clays. Geotechnique, 40(3): 329-378.

Çagatai, M.N., Keigwin, L.D., Okay, N., Sari, E., Algan, O., 2002. Variability of clay-mineral composition on Carolina Slope (NW Atlantic) during marine isotope stages 1-3 and its paleoceanographic significance. Marine Geology, 189: 163-174.

Christidis, G.E., 1998. Physical and chemical properties of some bentonite deposits of Kimolos Island, Greece. Applied Clay Science, 13(2): 79-98.

Cole, T.G., Shaw, H.F., 1983. The nature and origin of authigenic smectites in some recent marine sediments. Clay Mineralogy, 18: 239-252.

Colombo, P., Colleselli, F., 1996. Elementi di geotecnica. Zanichelli, Bologna, Italy.

Diegel, F.A., Karlo, J.F., Schuster, D.C., Shoup, R.C., Tauvers, P.R., 1995. Cenozoic structural evolution and tectono-stratigraphic framework of the northern Gulf Coast Continental Margin. In: M.P.A. Jackson, D.G. Roberts and S. Snelson (Eds.), Salt tectonics: a global prospective. AAPG Memoir 65, pp. 109-151.

Dixon, J.B., Weed, S.B., 1989. Minerals in soil environments -2nd edition. SSSA Book Series. SSSA, Madison, WI, 1244 pp.

Dixon, J.B., White, G.N., 1999. Soil mineralogy laboratory manual (5th edition). Pub. by the authors, Dep. of Soil and Crop Sciences, Texas A&M University, College Station, TX

Folk, R., 1974. Techniques in grain size analysis, Petrology of Sedimentary Rocks. Hemphill Publishing Co., Austin, TX, pp. 16-53.

Foucault, A., Melier, F., 2000. Paleoclimatic cyclicity in central Mediterranean Pliocene sediments: the mineralogical signal. Palaeogeography, Palaeoclimatology, Palaeoecology, 158: 311-323.

Grabowska-Olszewska, B., 2003. Modelling physical properties of mixtures of clays: example of a two-component mixture of kaolinite and montmorillonite. Applied Clay Science, 22(5): 251-259.

Griffin, G.M., 1962. Regional clay-mineral facies -Products of weathering intensity and current distribution in the northeastern Gulf of Mexico. GSA Bulletin, 73: 737-768.

Harder, H., 1974. Illite mineral synthesis at surface temperatures. Chemical Geology, 14(4): 241-253.

Holtz, R.D., Kovacs, W.D., 1981. An introduction to geotechnical engineering. Prentice-Hall, Inc., Englewood Cliffs, NJ.

Hottman, W.H., 1975. Areal distribution of clay minerals and their relationship to physical properties, Gulf of Mexico, Ph.D. Dissertation, Texas A&M University, College Station.

Jackson, M.L., 1956. Soil chemical analysis- advanced course. Pub. by the author, Dept. of Soils, University of Wisconsin, Madison, WI.

Jacobs, M.B., 1974. Clay mineral changes in Antarctic deep-sea sediment and cenozoic climatic events. Journal of Sedimentary Petrology, 44(4): 1079-1086.

Kahle, M., Kleber, M., Jahn, R., 2002. Review of XRD-based quantitative analyses of clay minerals in soils: the suitability of mineral intensity factors. Geoderma, 109: 191-205.

Kennett, J.P., Huddleston, P., 1972. Late Pleistocene paleoclimatology, foraminiferal biostratigraphy and tephrochronology, western Gulf of Mexico. Quaternary Research, v.2, p.38-69.

Kump, L.R., Brantley, S.L., Arthur, M.A., 2000. Chemical weathering, atmospheric CO_2, and climate. Annual Review of Earth Planetary Science, 28: 611-667.

Ishizuka, T., Kawahata, H., Aoki, S., 1986. Interstitial water geochemistry and clay mineralogy of the Mississippi fan and Orca and Pigmy Basins, Deep Sea Drilling Project Leg 96. In: Bouma, A. H., Coleman, J. M., Mayer, A. W., et al. (Eds.). Initial Reports of the Deep Sea Drilling Project. Government Printing Office, Washington, DC, pp.711-728.

Lambe, T.W., 1960. A mechanistic picture of shear of shear strength in clay. In: Proceedings of the Research Conference on Shear Strength of Cohesive Soils, Boulder, CO, p.555-580

LaRosa, P.T., 2000. Identification of mass wasting using stress state on basin slope in northwestern Gulf of Mexico, M.S. Thesis, University of Rhode Island, Narragansett.

Lauer-Laredde, C., Pezard, P.A., Robert, C., Dekeyser, I., 1998. Mineralogical association and physical properties of sediments with paleoclimatic implications (ODP site 798B, Japan Sea): a comparative study from core and downhole measurements. Marine Geology, 150: 73-98.

Lee, G.H., Watkins, J.S., Bryant, W.R., 1996. Bryant Canyon fan system: an unconfined, large river-sourced system in the northwestern Gulf of Mexico. AAPG Bulletin, 80(3): 340-358.

Leigh, D.S., 1994. Roxana silt of the Upper Mississippi Valley: lithology, source, and paleoenvironment. GSA Bulletin, 106: 430-442.

Liu, J.Y., Bryant, W.R., 2000. Sea floor morphology and sediment paths of the northern Gulf of Mexico deepwater. In: A.H. Bouma and C.G. Stone (Eds.), Fine-grained turbidite systems, AAPG Memoir 72/SEPM Special Publication 68, pp. 33-46.

Lumsden, D.N., 1988. Characteristics of deep-marine dolomite. Journal of Sedimentary Petrology, 58(6): 1023-1031.

Ma, C., Eggleton, R.A., 1999. Cation exchange capacity of kaolinite. Clays and Clay Minerals, 47(2): 174-180.

Mathew, P., d Rao, S.N., 1997. Influence of cations on compressibility behavior of a marine clay. Journal of Geotechnical and Geoenvironmental Engineering, 123(11): 1071-1073.

Michalopoulos, P., Aller, R., 1995. Rapid clay mineral formation in Amazon delta sediments: reverse weathering and oceanic elemental cycles. Science, 270: 614-617.

Milne, I.H., Earley, J.W., 1958. Effect of source and environment on clay minerals. AAPG Bulletin, 42(2): 328-338.

Mitchell, J.K., 1993. Fundamentals of soil behavior. John Wiley & Sons, Inc., New York, 437 pp.

Moore, D.M., Reynolds, R.C.J., 1989. X-ray diffraction and the identification and analysis of clay minerals. Oxford University Press, Oxford, 332 pp.

Ohtsubo, M., Egashira, K., Tanaka, H., Mishima, O., 2002. Clay minerals and geotechnical index properties of marine clays in East Asia. Marine Georesources and Geotechnology, 20(4): 223-246.

Pandian, N.S., Nagaraj, T.S., 1990. Critical reappraisal of colloidal activity of clays. Journal of Geotechnical Engineering, 116(2): 285-295.

Petit, S., Righi, D., Madejova, J., Decarreau, A., 1998. Layer charge estimation of smectites using infrared spectroscopy. Clay Mineralogy, 33: 579-591.

Post, J.L., Borer, L., 2002. Physical properties of selected illites, beidellites and mixed-layer illite-beidellites from southwestern Idaho, and their infrared spectra. Applied Clay Science, 22(3): 77-91.

Prather, B.E., 2000. Calibration and visualization of depositional process models for above-grade slopes: a case study from the Gulf of Mexico. Marine and Petroleum Geology, 17: 619-638.

Prather, B.E., Booth, J.R., Steffens, G.S., Craig, P.A., 1998. Classification, lithologic calibration, and stratigraphic succession of seismic facies of intraslope basins, deep-water Gulf of Mexico. AAPG Bulletin, 82(5A): 701-728.

Reynolds, R.C.J., 1985. NEWMOD©, a computer program for the calculation of one dimensional diffraction patterns of mixed-layered clays. Pub. by the author, Dep. of Earth Science, Dartmouth College, Hanover, NH.

Reynolds, R.C.J., 1989. Diffraction from small and disordered crystals. In: D.L. Bish and J.E. Post (Eds.), Modern powder diffraction. Mineralogical Society of America, Washington, DC, pp. 145-182.

Robert, C., Chamley, H., 1991. Development of early Eocene warm climate, as inferred from clay mineral variations in oceanic sediments. Palaeogeography, Palaeoclimatology, Palaeoecology, 89: 315-331.

Robert, C., Kennett, J.P., 1994. Antarctic subtropical humid episode at the Paleocene-Eocene boundary: clay mineral evidence. Geology, 22: 211-214.

Scafe, D.W.,1968. A clay mineral investigation of six cores from the Gulf of Mexico. Ph.D. Dissertation, Texas A&M University, College Station, TX

Seed, H.B, Woodward, R.J., Lundgren, R., 1964. Clay mineralogical aspects of the Atterberg limits. Journal of Soil Mechanics and Foundations Division, ASCE, 90(SM4), p.107-131.

Skempton, A.W., 1970. The consolidation of clays by gravitational compaction. Quarterly Journal Geological Society of London, 125(499): 373-411.

Smith, J.V., Gay, P., 1958. The powder patterns and lattice parameters of plagioclase feldspars, II. Mineralogical Magazine, 31: 744-762.

Sridharan, A., Jayadeva, M.S., 1982. Double layer theory and compressibility of clays. Geotechnique, 32(2): 133-144.

Sridharan, A., Prakash, K., 1999. Mechanisms controlling the undrained shear strength behavior of clays. Canadian Geotechnical Journal, 36: 1030-1038.

Sridharan, A., Rao, S.M., Murthy, N.S., 1988. Liquid limit of kaolinitic soils. Geotechnique, 38(2): 191-198.

Sridharan, A., Rao, S.M., Murthy, N.S., 1986. Liquid limit of montmorillonite soils. Geotechnical Testing Journal, 9(3): 156-159.

Stearns, S.V., 1985. Incipient diagenesis of sediments from the Pigmy Basin, Northern Gulf of Mexico. M.S. Thesis. Texas A&M University, College Station, TX.

Tieh, T. T., Stearns, S., Presley, B. J., 1986. Mineralogy and incipient diagenesis of Pigmy Basin sediments, Hole 619, Deep Sea Drilling Project Leg 96. In: Bouma, A. H., Coleman, J. M., Mayer, A. W., et al. (Eds.). Initial Reports of the Deep Sea Drilling Project. Government Printing Office, Washington, DC, pp.577-585.

Thiry, M., 1999. Paleoclimatic interpretation of clay minerals in marine deposits: an outlook from the continental margin. Earth Science Reviews, 49: 201-221.

Thomas, P.J., Baker, J.C., Zelazny, L.W., 2000. An expansive soil index for predicting shrink-swell potential. Soil Science Society of America Journal, 64: 268-274.

Tompkins, R.E., Shephard, L.E., 1979. Orca basin: depositional processes, geotechnical properties and clay mineralogy of Holocene sediment within an anoxic hypersaline basin, northwest Gulf of Mexico. Marine Geology, 33: 221-238.

Tripsanas, E.K., 2003. Evolution of sedimentological and slope instability processes on the Bryant Canyon area, northwest Gulf of Mexico, Ph.D. Dissertation, Texas A&M University, College Station, TX.

Tripsanas, E., Bryant, W.R., Berti, D., Silva, A.J., 2000. Sedimentological nature of the Bryant Canyon area, northwest Gulf of Mexico. AAPG Bulletin, 84(10):1692-1693.

Walker, J.R., 1993. An introduction to computer modeling of X-ray diffraction patterns of clay minerals: a guided tour of NEWMOD©. In: R.C.J. Reynolds and J.R. Walker (Eds.), Computer application to X-ray powder diffraction analysis of clay minerals. CMS Workshop Lectures. The Clay Mineral Society, Boulder, CO.

Weaver, C.E., 1977. The clay petrology of sediments. In: J.I. Drever (Editor), Sea water; cycles of the major elements. Dowden, Hutchinson and Ross., Stroudsburg, PA, pp. 125-140.

Wetzel, A., 1990. Interrelationships between porosity and other geotechnical properties of slowly deposited, fine-grained marine surface sediments. Marine Geology, 92: 105-113.

Whitehouse, U.G., McCarter, R.S., 1977. Diagenetic modification of clay mineral types in artificial sea water. In: J.I. Drever (Editor), Sea water; cycles of the major elements. Dowden, Hutchinson and Ross., Stroudsburg, PA, pp. 141-179.

APPENDIX A

CLAY MINERALS

Even though many minerals can be present in the clay fraction of siliciclastic sediments, just a few of them are responsible for the special properties of such a fraction and most often make up the majority of it. These minerals, referred to as clay minerals, belong to the phyllosilicate group, so called because its molecular structure is composed of SiO_2 tetrahedra linked together in a planar arrangement (Dixon and Weed, 1989). Tetrahedra sheets are bond to $Al^{3+}O_2(OH)$ or $M^{2+}O_2(OH)$ octahedra sheets in a 2:1 or 1:1 ratio, thus forming the basic layer of phyllosilicate minerals. In the 1:1 minerals, like kaolinite, layers are neutrally charged and they bond to each other by Van der Waals' forces that develop between surficial OH^- and O^{2-} of different layers. In 2:1 clays, partial isomorphous substitutions in tetrahedral or octahedral sites cause layers to be negatively charged. In these cases cations or ion complexes enter the interlayer region to counterbalance the charge (Fig. A1) (Dixon and Weed, 1989; Bennett, 1981).

Depending on the amount and location of isomorphous substitutions the layer charge varies along with the force acting on interlayer cations. The two extremes are represented by the mica and the smectite minerals (Dixon and Weed, 1989). In mica, tetrahedral substitutions are stechiometric (Al:Si=1:3) and cause a layer charge of -1, sufficient to hold K cations by strong ionic bonding. In smectite, the charge mostly originates from the octahedral sites, far from the surface, and varies between -0.6 and -0.3 per unit formula.

Because of the fractional charge, interlayer cations are weakly bonded and can be exchanged with surrounding solutions, furthermore the layer surface becomes hydrophilic and adsorbs water (Dixon and Weed, 1989).

Despite their structural similarity, mica and smectite behave quite differently due to their different surface properties. Clay mica has a less perfect structure than at coarser size, being characterized by lower K content, Al:Si deviating from 1:3, poorer crystallinity and higher water content. Due to these differences clay mica has a higher surface activity and may have a slightly incomplete charge distribution up to -0.9. The mica-smectite series also includes an intermediate member, vermiculite which by definition has interlayer charge ranging between -0.9 and -0.6. As expected, its properties are intermediate between those of mica and smectite.

Isomorphous substitution is not the only source of surface charge: broken bonds at the edges of particles and specific absorption also contribute to it. Charge caused by broken bonds is variable in character, its amount and sign being a function of pH (Dixon and Weed, 1989). The pH dependent charge has a stronger influence on minerals possessing a small permanent charge (Mitchell, 1976).

The dependence of clay volume change behavior on clay type and chemical environment is explained by the diffuse double layer theory (DDL). The theory predicts the distribution of the water molecules and the cations balancing clay surface negative charge (Van Olphen, 1977, Dixon and Weed, 1989). Cations and water are distributed in a diffuse layer surrounding the surface, whose thickness is determined by the balance of the surface

electric potential and cation charge. According to the Guyot-Chapman DDL the thickness of the diffuse double layer is:

$$t^2 = \Sigma kT / 8\rho z_i^2 e_i^2 n_i$$

Where: t = DDL thickness; k = Boltzman constant; T = temperature in K; ρ = density; z_i = charge of ion i; e_i = electric charge of ion i; n_i = concentration (Dixon and Weed, 1989)

The diffuse double layer opposes clay particle attraction, the thicker the layer the greater the tendency of clay particles to disperse and adsorb-absorb water. The DDL controls the sediment fabric and water retention potential which in turn affect sediment volume change behavior (Bennett, 1981). The Guyot-Chapman theory was later modified to account for other factors also affecting the DDL thickness, like ionic radius, ion hydration shells and specific absorption (Dixon and Weed, 1989).

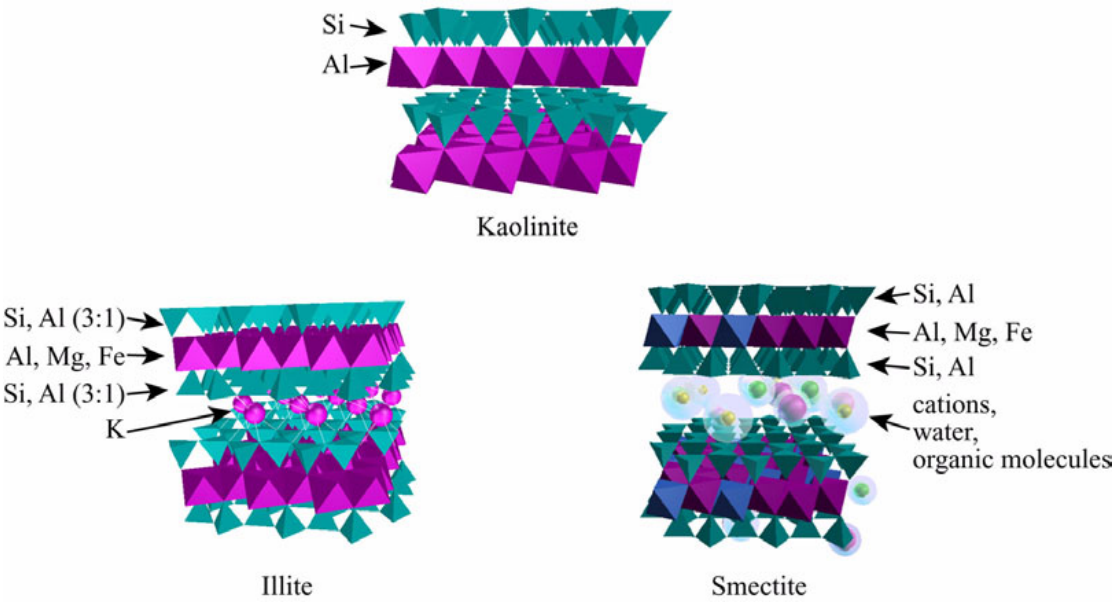

Fig. A1. Structures of kaolinite, illite and smectite represented as layers of tetrahedra and octahedra.

APPENDIX B

XRD PATTERNS

The XRD patterns correspond to the following treatments: a) Mg saturation at 25 ^{o}C; b) Mg saturation and glycerol solvation; c) K saturation at 25 ^{o}C; d) K saturation at 300 ^{o}C; e) K saturation at 550 ^{o}C.

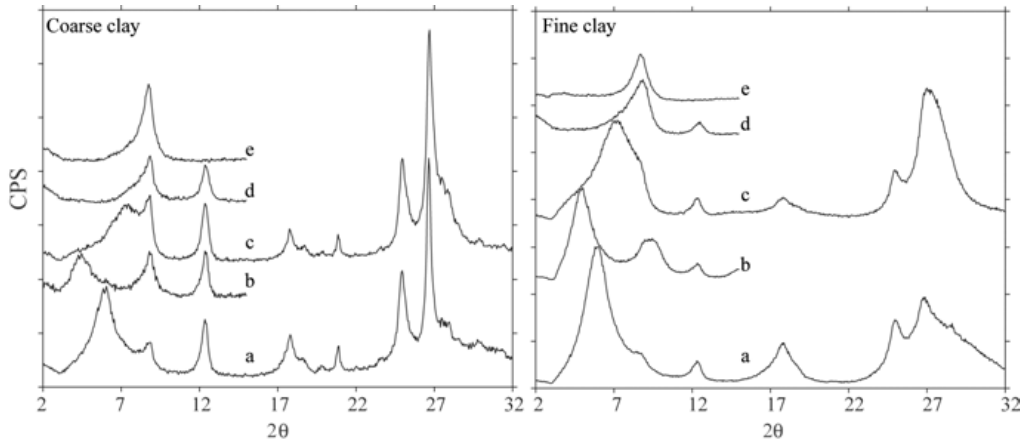

Fig. A2. Sample 31-1

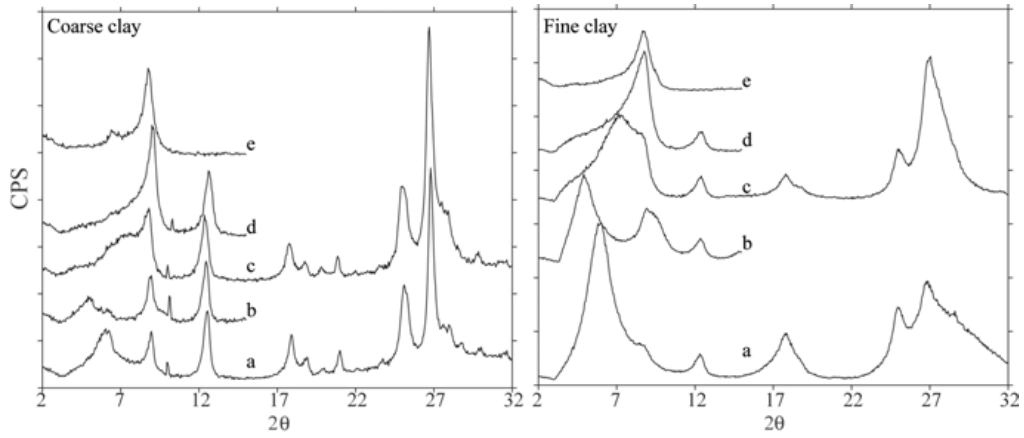

Fig. A3. Sample 31-2

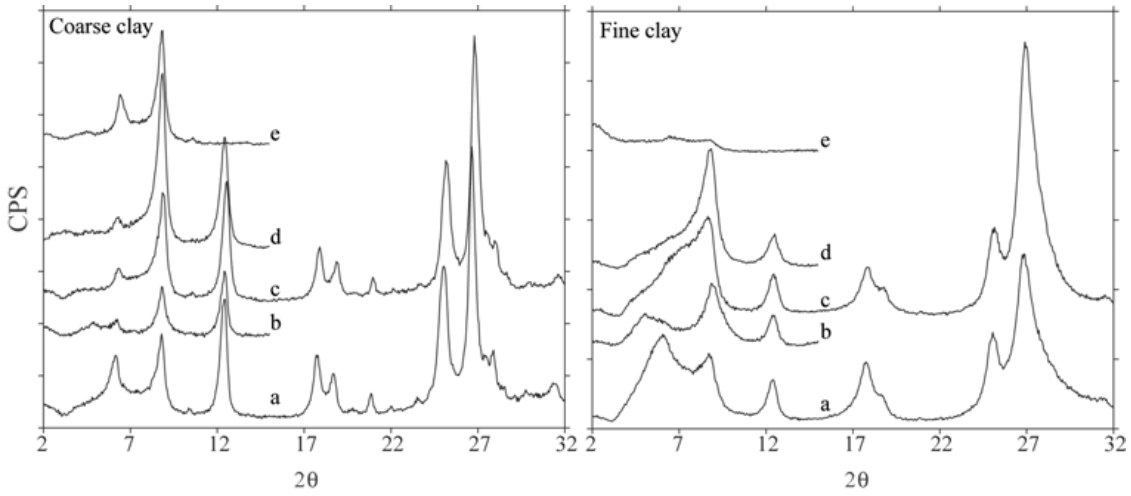

Fig. A4. Sample 31-3

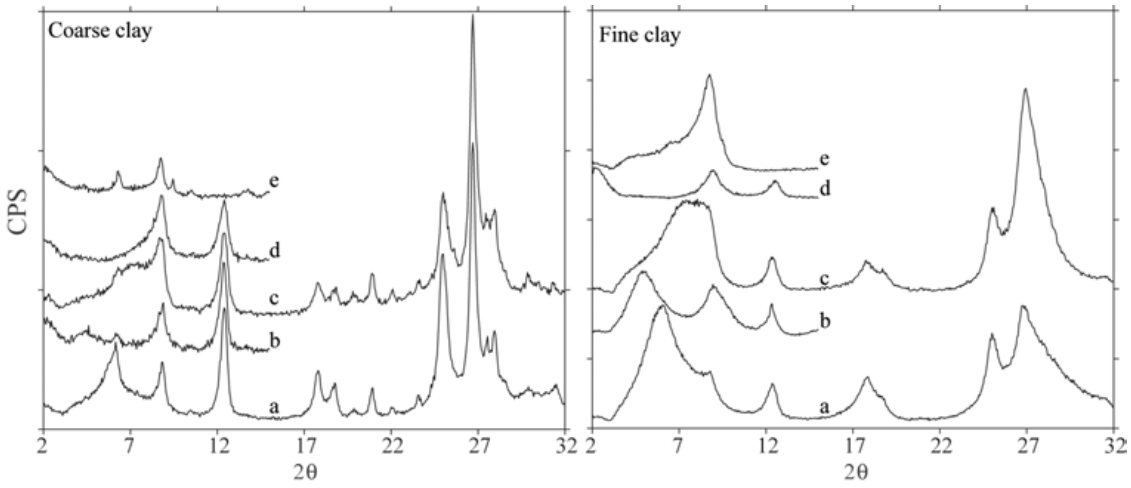

Fig. A5. Sample 31-4

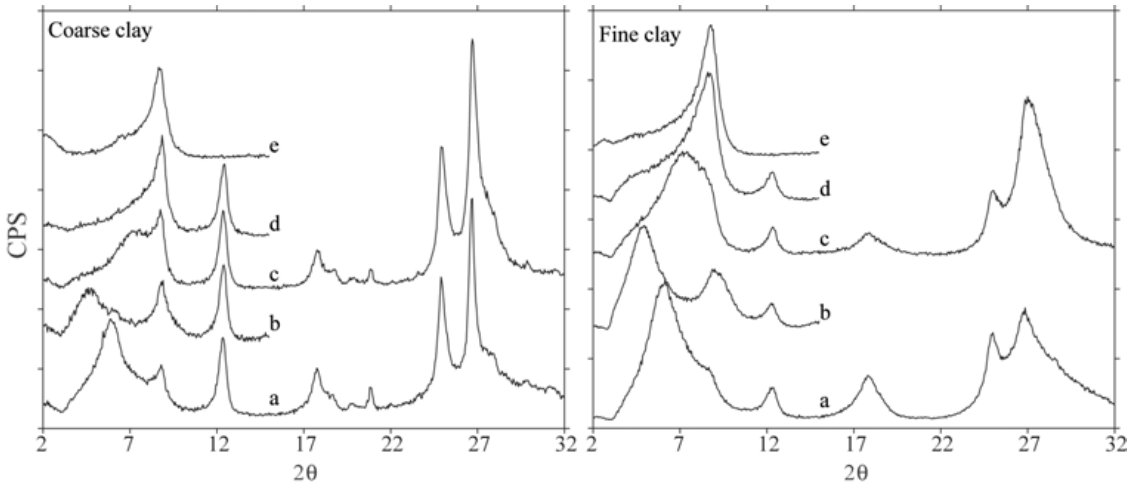

Fig. A6. Sample 31-5

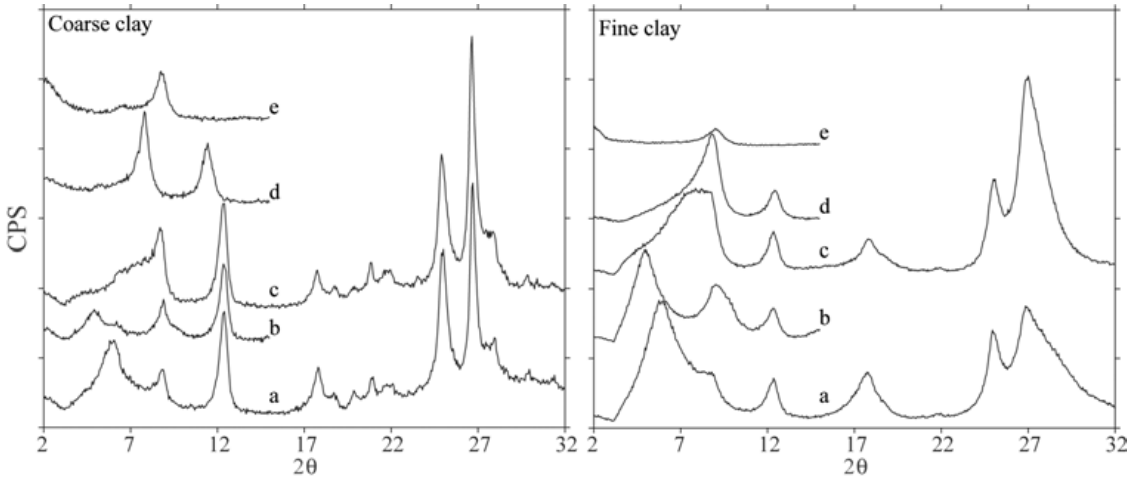

Fig. A7. Sample 31-6

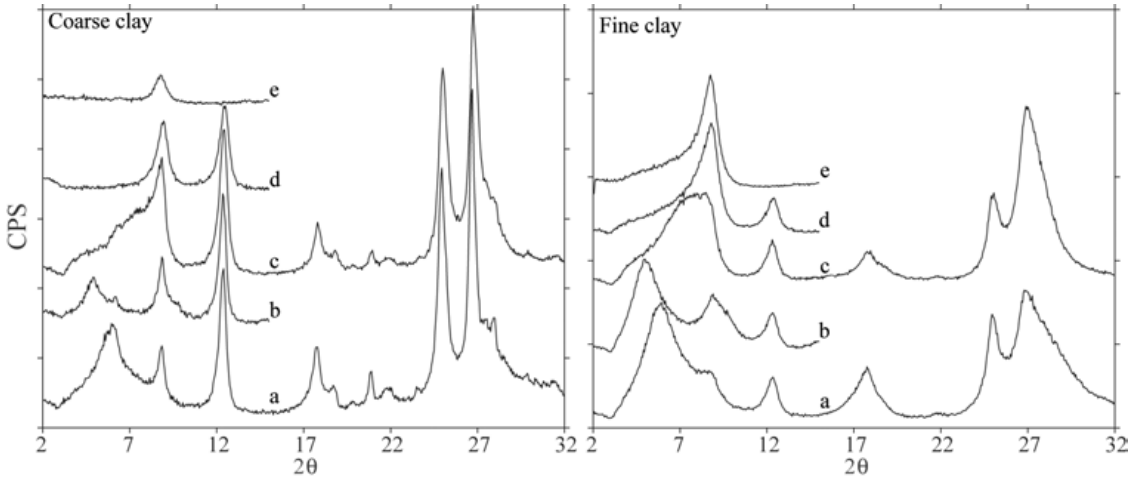

Fig. A8. Sample 31-7

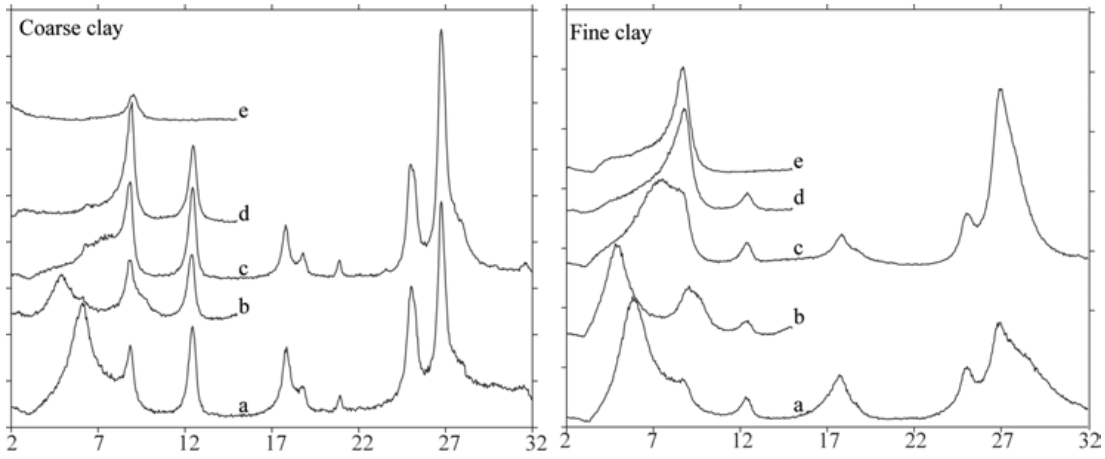

Fig. A9. Sample 33-1

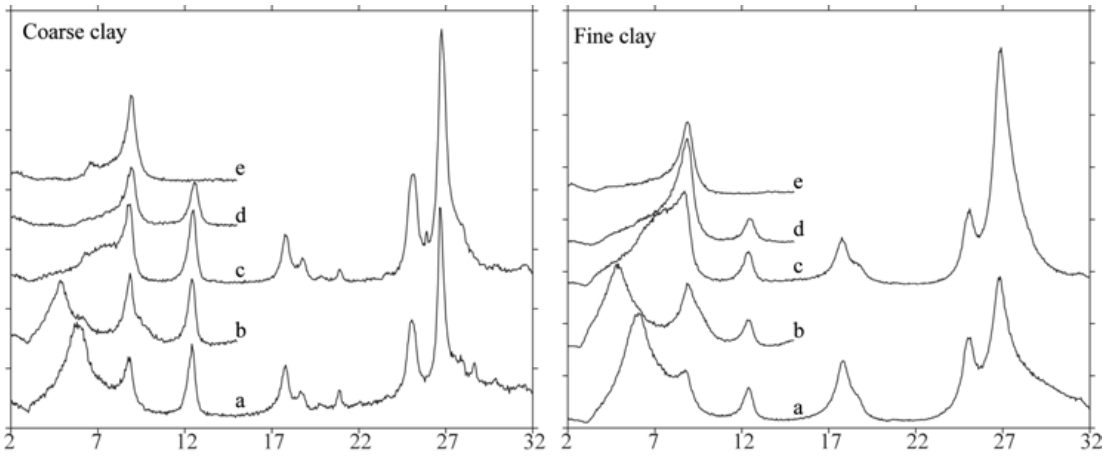

Fig. A10. Sample 33-2

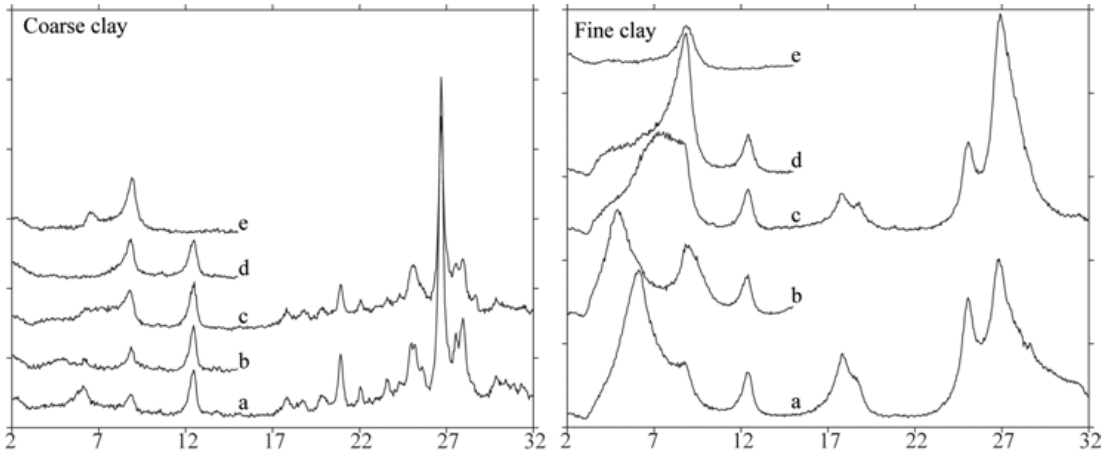

Fig. A11. Sample 33-3

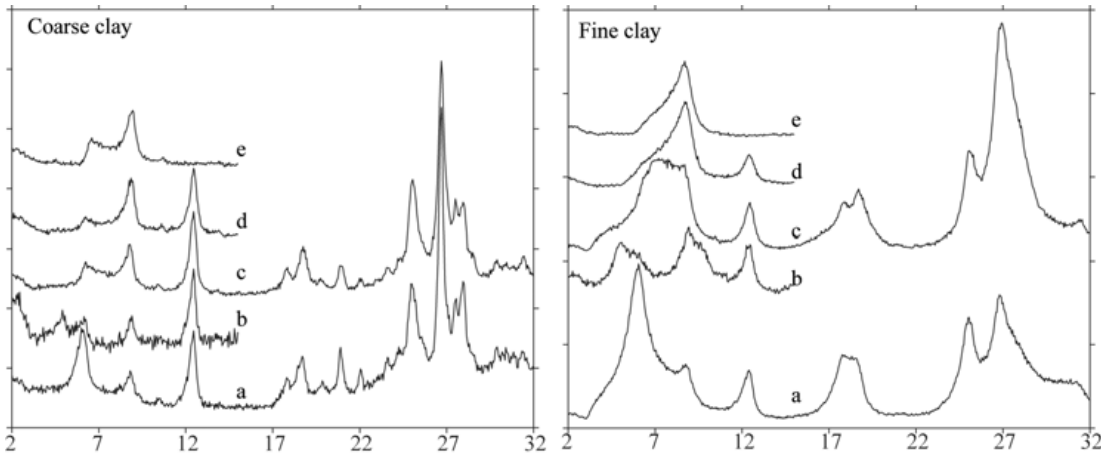

Fig. A12. Sample 37-1

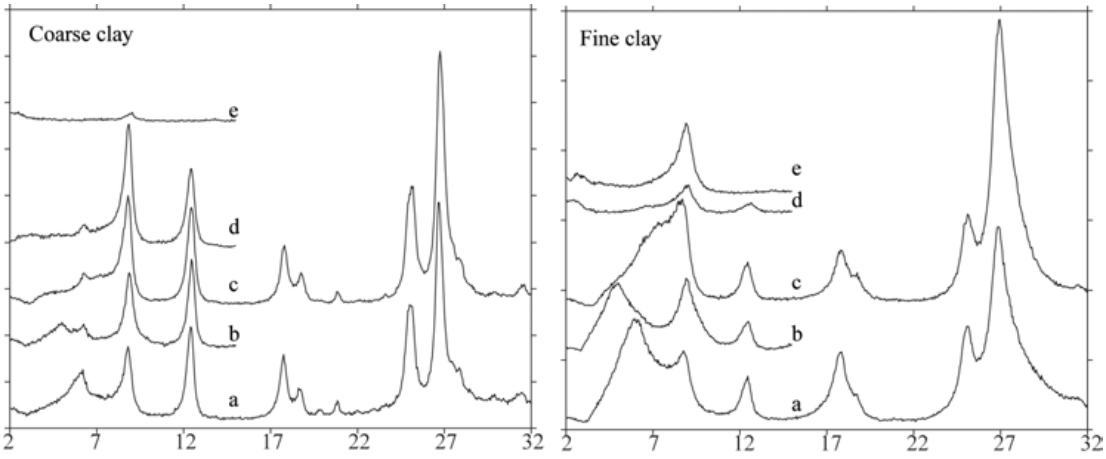

Fig. A13. Sample 46-1

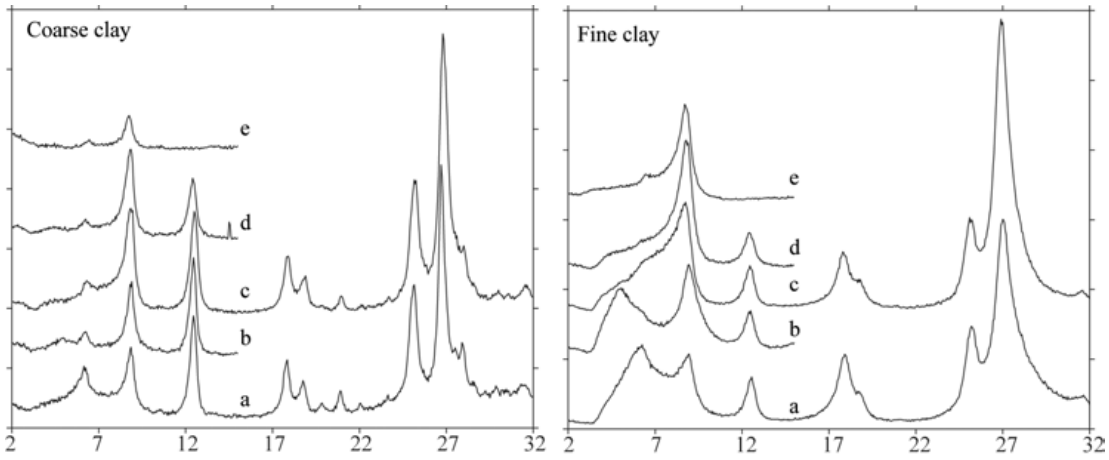

Fig. A14. Sample 46-2

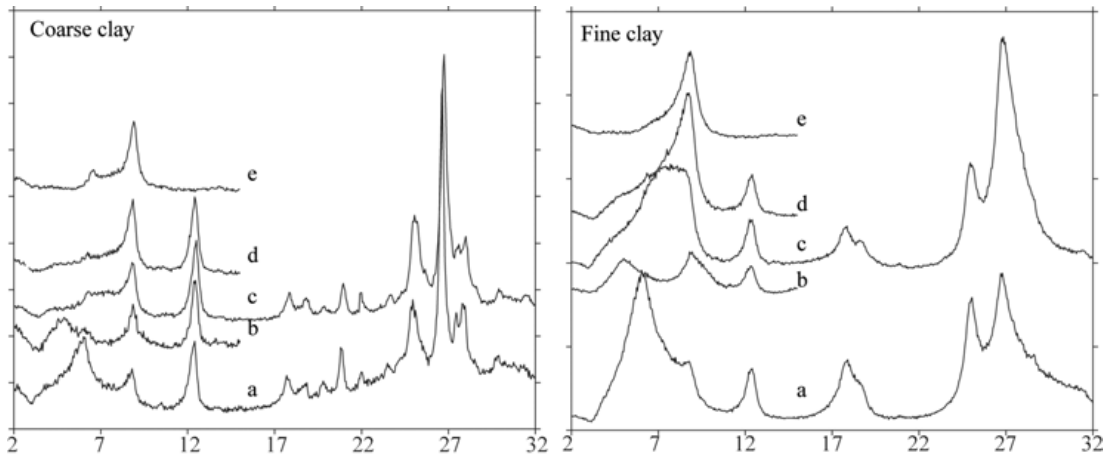

Fig. A15. Sample 46-3

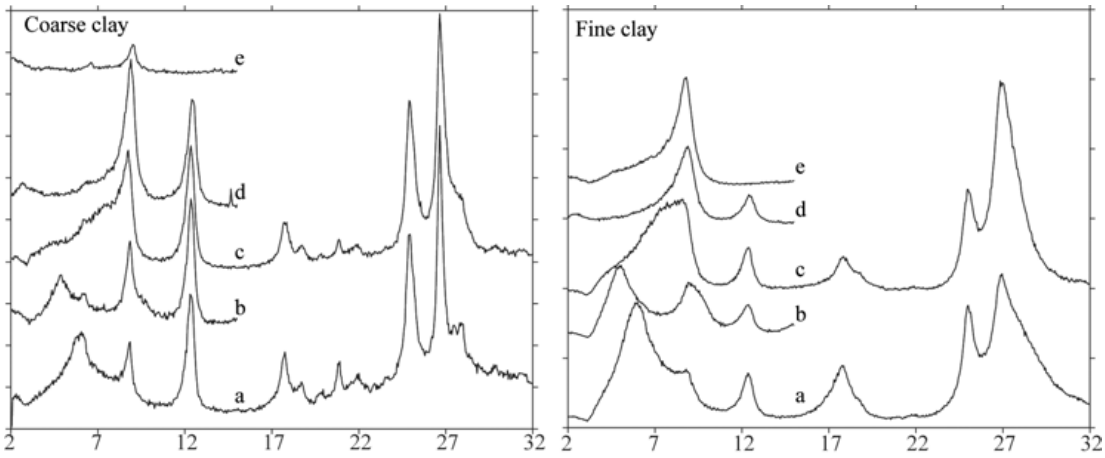

Fig. A16. Sample 46-4

APPENDIX C

INDEX PROPERTY DERIVATION FROM BULK DENSITY

Void ratio (e), porosity (n) and water content (W_C) are interdependent variables that can be calculated from bulk density (ρ_b) in saturated sediment, as long as grain density (ρ_S) is known or assumed and the density of the pore fluids are known. The equations and assumptions applied in this study are as follows.

Porosity is defined as the ratio between volume of the fluid and total volume, generally expressed in percent.

Cores used in this study were completely saturated with salt water (no gas was found) which has a density (ρ_W) of 1.024 g/cm^3. A grain density (ρ_S) of 2.71 g/cm^3 was assumed for these sediments based on measurements conducted at URI (LaRosa, 2000). Based on these grain density and water density values, porosity was calculated according to Boyce (1976).

Void ratio is defined as the ratio between the volume of the voids and the volume of the solid fractions. It is related to porosity by the following equation:

$e = (1/100)*n/(1-n)$

Finally, water content is defined as the weight of the water divided by the dry weight of solids expressed as percentage. It can be derived from void ratio, assuming 100 % saturation, according to the following equation:

$W_C = 100*(\rho_W/\rho_S)*e$

VITA

DEBORA BERTI
Department of Oceanography
Texas A&M University
College Station, TX 77843
email: debora@ocean.tamu.edu

EDUCATION

Texas A&M University, College Station
M.S. in Geological Oceanography — December 2003

Bologna University, Bologna, Italy
Laurea in Geological Science — December 1999
Thesis title: Geologic study for the stabilization of the town of Gabicce (Italy)

EXPERIENCE

Oceanography Department, Texas A&M University
Graduate Research Assistant — 1999 to Present

FIELD EXPERIENCE

D/V JOIDES Resolution, ODP Leg 207 (Demerara Rise)
Physical Property Specialist — January-March 2003

R/V Moana Wave (Hawaii)
Participantin a gravity coring cruise — May 1999

R/V Gyre (Gulf of Mexico)
Participant in a deep-towed seismic cruise — March 1999

PUBLICATIONS

Berti, D., Bryant, W.R., 2001. Geotechnical properties of the Bryant Canyon, Northwest Gulf of Mexico continental slope. In: Proc. of OTRC 2001 Int. Conf. honoring Prof. Wayne Dunlap. C. Aubeny and J.L. Briaud ed., College Station, TX

Tripsanas, E.K., Berti, D., Bryant, W.R., Bean, D.A., Liu, J.Y., Meyer, M, Phaneuf, B., 2000. Sedimentological characteristics of the lower continental slope in the Bryant Canyon area, Northwest Gulf of Mexico. EOS, Transactions of the American Geophysical Union, 80 (49 / Supplement), OS186.